D2.2 Definition of system context and limits for use

Authors: Carlos Ochoa (IERC), Andreea LeCam (IERC), Ruchi Agrawal (IERC), Georgios Zisopoulos (CERTH), Athanasios Nesiadis (CERTH), Alexandros Tsimpoukis (CERTH), Georgios Martinopoulos (CERTH), Nikolaos Nikolopoulos (CERTH), Philipp Schuetz (HSLU), Robert Gandia (HSLU), Driss Stitou (CNRS), Alberto Belda (CARTIF), Roberto Arnanz (CARTIF), Marco Rocchetti (R2M)

This project has received funding from the European Union's Horizon 2020 research and innovation programme under grant agreement No 869821

D2.2 Definition of system context and limits for use

Summary

This deliverable presents the main context for application of the MiniStor system, helps to define the requirements to be met by the system at both the technical and marketing level. It includes a brief study of climate distribution across the continent in terms of Koppen-Geiger classification and Heating and Cooling Degree Days (HDD and CDD). It also provides an overview of resource availability such as solar radiation across the European continent. Relevant building characteristics were studied using features that must be taken into account for technical development of the system, such as building typologies, useful areas, etc. Sources such as Eurostat and other European research projects were consulted for information on this subject. The impact of users on energy demand and consumption was studied through definition of energy profiles, which include their occupancy of a space, type of activities performed, and equipment that is involved in performing those activities, including lighting. Sources for these elements come from relevant professional guidelines and accepted values.

Deliverable Number	Work Package
D2. 2	WP 2
Lead Beneficiary	**Deliverable Author(S)**
International Energy Research Centre - Tyndall National Institute-University College Cork (IERC)	Carlos Ochoa (IERC), Andreea LeCam (IERC), Ruchi Agrawal (IERC), Georgios Zisopoulos (CERTH), Athanasios Nesiadis (CERTH), Alexandros Tsimpoukis (CERTH), Georgios Martinopoulos (CERTH), Nikolaos Nikolopoulos (CERTH), Philipp Schuetz (HSLU), Robert Gandia (HSLU), Driss Stitou (CNRS), Alberto Belda (CARTIF), Roberto Arnanz(CARTIF), Marco Rocchetti (R2M), Federica Franzè (R2M)
Beneficiaries	**Deliverable Co-Author (S)**
EndeF	Adriana Coca Ortegon
Planned Delivery Date	**Actual Delivery Date**
30/04/2020	20/08/2024 3rd Revised Version

Type of deliverable	R	Report	X
Dissemination Level	CO	Confidential, only for members of the consortium (including the Commission)	
	PU	Public	X

This project has received funding from the European Union's Horizon 2020 research and innovation programme under grant agreement No 869821

Index

List of Tables

List of Images

List of Abbreviations and Acronyms

ASHRAE	American Society of Heating, Refrigerating and Air-Conditioning Engineers
CDD	Cooling Degree Days
DD	Degree-Day
EU	European Union
EPBD	Energy Performance of Buildings Directive (EU)
GCM	Global Climate Model
GDD	Growing Degree Days
GIS	Geographical Information Systems
HDD	Heating Degree Days
IPCC	Intergovernmental Panel on Climate Change
kWh	kilowatt-hour
kWh/K	kilowatt-hour per degree Kelvin degree
kWh/m^2	kilowatt-hours per square meter
lm/W	lumen per watt
m^2	square meter
Mtoe	Million Tonnes of Oil Equivalent
nZEB	nearly -Zero Energy Building
Ppm	parts per million
PVGIS	Photovoltaic Geographical Information System
PVT	Photovoltaic Thermal (hybrid solar panels)
RCM	Regional Climate Model
RCP	Representative Concentration Pathways
TMY	Typical Meteorological Year
WP	Work Package
W/m^2	watt per square meter

1 Introduction

The main objective of this deliverable is to define the context where the energy storage system will be applied. This will help define the requirements to be met by the system in terms of climate, architecture and infrastructure needed for its functioning. A comprehensive study of the current situation is needed, since buildings represent approximately 40% of the EU final energy consumption but characteristics of this consumption are diverse.

Almost two thirds of this consumption, which reached 458 Mtoe in 2016, concern the residential sector. Even tough household energy efficiency has improved by 28% in EU since 2000, energy consumption has only slightly decreased. This due to improvements in efficiency being counterbalanced by a growing number of dwellings together with increased demand per dwelling (Rousselot, 2018), amounting to an annual average consumption of 170 kWh/m^2. However, this figure is not uniform, and large disparities in energy consumption across EU countries can be attributed mainly to climate conditions and building characteristics. Approximately two thirds of this energy is consumed in order to cover space heating needs. Therefore, improving the efficiency of residential heating systems would contribute significantly to the energy consumption decrease and the reduction of corresponding greenhouse gases emissions, which is one of the primary targets of the European Union Energy Policy.

The deliverable contains studies into the classification of climate parameters according to weather patterns, heating and cooling demands, as well as availability in the European area of solar radiation needed to power Photovoltaic Thermal (PVT) panels. Building typologies and types of heating systems are also detailed. The influence of loads and users are taken into account through the study of different heat gains and user occupancies.

Sources consulted for this study include the European housing census, databases for solar availability, for heating and cooling demand, and publications from professional bodies such as ASHRAE, CEN and SIA.

Studying these influencing factors will result in facilitating the integration of the proposed system within the building, serving as basis for component calculations (WPs 3, 4, 5). This deliverable will also provide a first overview of parameters that need to be taken into account for market analysis and circular economy models (WP7).

2 Classification of Climate Zones

The proposed climate zoning takes into account the Köppen-Geiger climate classification, together with heating and cooling degree days. These parameters were chosen as they are some of the most used methods defining the climatic conditions of regions, and also because there is a good correlation between geographical location, type of climate and the corresponding heating and cooling degree days. This combined method considers not only weather patterns that can affect need for heating and cooling, but also helps quantify those needs in a preliminary way.

2.1 Köppen-Geiger climate classification

An overall classification of climate zones is useful to provide an overview of availability of natural resources such as direct sunlight availability and temperature distribution during the year. There are different methods of classifying the climatic zones of the world, with the most widespread climate classification method is the Köppen-Geiger classification (Kottek, 2006).

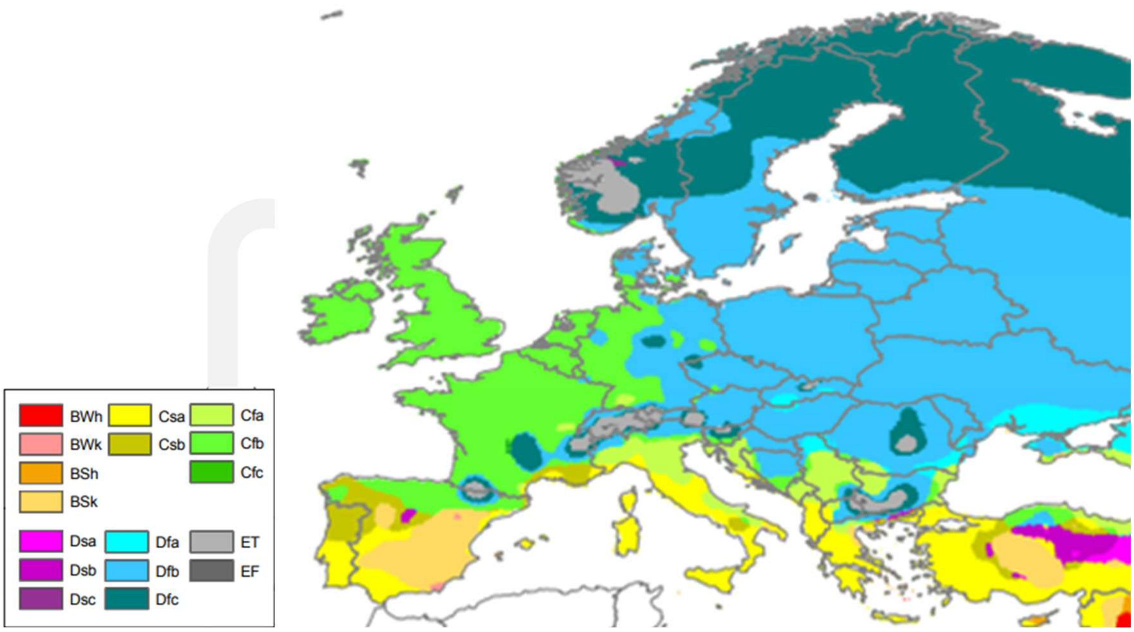

Fig 1: Köppen-Geiger climate map of Europe. Source: Peel et al. 2007

There are 30 possible climate types according to features such as mean annual temperature, annual precipitation and its distribution during the year. They are coded according to letters, with the positions of these letters representing features of the climate types. The five main climate groups are described through the first letter as: (A) tropical zone, (B) arid zone, (C) temperate zone, (D) cold zone, and (E) polar zone. A second letter is used to describe the level of precipitation and a third letter defines a dominating attribute of air temperature. For example, Csa defines the temperate climate with dry summer, while Cfa defines a temperate, fully humid climate with hot summers. The model, however, can only be used to define very large areas and is not accurate for transition zones. Figure 1 shows the map of Europe with the different climatic zones defined by the Köppen-Geiger climate classification (Peel et al., 2007).

When applied to the demonstration sites, it can be seen that by area distribution countries like Hungary and Ireland have one predominant climate type, while Spain and Greece have a predominant climate with several microclimates. Boundaries between climate zones are not straightforward and some overlaps can occur.

The demo sites for the MiniStor project are based in continental Spain (Santiago del Compostela), Hungary (Sopron), Greece (Thessaloniki and Kimmeria) and Ireland (Cork). The following table shows the different climate zones for the countries where the demo sites are located, and the percentage covered by such zone.

Country	% of country surface	Climatic zone nomenclature	Definition of climatic zone
Spain	20	Cfb	Temperate, without dry season, warm summer
	45	BSk	Arid, steppe, cold
	10	Csb	Temperate, with dry and warm summer
	25	Csa	Temperate, with dry and hot summer
Greece	80	Csa	Temperate, with dry and hot summer
	10	BSk	Arid, steppe, cold (high mountain ranges, like Pindus and Rhodope)
	5	Csb	Temperate, with dry and warm summer
	5	Dsa	Cold, dry and hot summer
Hungary	100	Dfb	Cold, without dry season, warm summer
Ireland	100	Cfb	Temperate, without dry season, warm summer

Table 1: Definition of main climatic zones for the countries with the demo sites

2.2 Heating and Cooling Degree Days

Although the Köppen-Geiger classification is useful to define broad characteristics for each climate that can affect the variability of renewable energy sources, it cannot reflect the energy demands for each location.

In order to quantify such needs, heating and cooling degree days are used. They characterize the difference between a daily mean and an outside base temperature where it is considered heating or cooling are not necessary. Different countries and regions use different base temperatures that can take into account the effect of insulation or thermal comfort.

A degree-day is a quantity that denotes the extremity and duration of ambient temperature. In general, it is defined as the deviation of the latter from a reference temperature, known as base temperature (CIBSE, 2006). The most used degree days are: a) Heating Degree Days (HDD), b) Cooling Degree Days (CDD) and c) Growing Degree Days (GDD) (Spinoni et al., 2015). The latter type is used in phenology, whereas Heating and Cooling Degree Days are applied in estimations of the energy consumption in buildings, as the heat exchange between a building and the environment is predominantly proportional to the difference between the indoor and outdoor temperatures. Consequently, HDD and CDD are related to heating and cooling energy demands respectively. Additionally, these variables are widely used as indicators of the global warming impact on the future building energy needs (Mourshed, 2012).

There are various methods that can be utilized in order to calculate the HDD and CDD variables. The hourly method is considered as the most accurate, since the deviation from the base temperature is calculated at every hour of the day (Mourshed, 2012). However, it requires the utilization of hourly ambient temperature values, which are not possible to be provided in many cases. In this analysis, the American Society of Heating, Refrigerating and Air-Conditioning (ASHRAE) daily mean method is used, which requires only the knowledge of the daily mean temperature (ASHRAE, 2017). Therefore, it is suitable for performing current and future energy estimations, since latter projections of only the daily mean temperature are available.

2.2.1 ASHRAE Method

According to the ASHRAE daily mean temperature method, the value of degree-days of each day is equal to the difference between the daily mean temperature T_{daily} and the base temperature T_{base} (Mourshed, 2012). Equations (1) and (2) describe the calculation of HDD and CDD respectively.

$$HDD_{daily}=(T_{base} - T_{daily})^{+} = (T_{base} - T_{daily}) \cdot \theta(T_{base} - T_{daily}) \quad (1)$$

$$CDD_{daily}=(T_{daily} - T_{base})^{+} = (T_{daily} - T_{base}) \cdot \theta(T_{daily} - T_{base}) \quad (2)$$

The symbol "+" in the above equations indicate that only positive differences of the corresponding variables are considered. The daily mean temperature T_{daily} is calculated as the average of daily maximum and minimum ambient temperatures T_{max} and T_{min} respectively:

$$T_{daily} = \frac{T_{max}+T_{min}}{2} \quad (3)$$

In the framework of this analysis the values of monthly, monthly mean, annual and annual mean degree days are also calculated. Monthly degree-days $HDD_{monthly}$ and $CDD_{monthly}$ are calculated by summing up the daily degree-days in a month, whereas $HDD_{monthly\_mean}$ and $CDD_{monthly\_mean}$ are the monthly mean values and represent the average daily values within a month.

$$HDD_{month} = \sum_{i=1}^{M}(HDD_{daily,i}) \quad (4)$$

$$CDD_{monthly} = \sum_{i=1}^{M}(CDD_{daily,i}) \quad (5)$$

$$HDD_{month\_mean} = {HDD_{monthly}}/{M}$$

(4)

$$CDD_{monthly\_mean} = {CDD_{monthly}}/{M} \quad (5)$$

where M is the number of days in a month and $DD_{daily,I}$ is the value of daily degree-days on the i^{th} day of the month.

Annual degree-days, HDD_{annual} and CDD_{annual} are calculated by summing up the monthly degree-days:

$$HDD_{annual} = \sum_{j=1}^{12}(HDD_{monthly,j}) \quad (8)$$

$$CDD_{annual} = \sum_{j=1}^{12}(CDD_{monthly,j}) \quad (9)$$

where $DD_{monthly,j}$ is the value of the monthly degree-days in the j^{th} month of the year.

Finally, annual mean degree-days, HDD_{annual_mean} and CDD_{annual_mean} are calculated as the average of the twelve monthly mean degree-days:

$$HDD_{annual\_mean} = \frac{HDD_{annual}}{365} \quad (10)$$

$$CDD_{annual\_mean} = \frac{CDD_{annual}}{365} \quad (11)$$

2.2.2 Selection of base temperature

The value of the base temperature affects considerably the resulting HDD and CDD, and consequently the accuracy of building energy needs' estimations. The selection should take into consideration local weather conditions (humidity, wind regime etc.) as well as specific building characteristics (size, insulation used etc.) (Kadioğlu et al., 2001). Therefore, there are no universally accepted base temperatures and many studies can be found in the literature that concern neighbouring countries where different base values are adopted. Additionally, the base temperatures used for HDD calculations might differ from those used for CDD calculations. In the current analysis distinct base temperatures for each demo site are selected based on literature (Azevedo et al., 2015, Skarbit et al., 2017, Wikipedia, Papakostas et al., 2010). They are depicted in the following table:

Location	Base Temperature for HDD	Base Temperature for CDD
Cork Ireland (Azevedo et al., 2015)	18°C	18°C
Santiago de Compostela Spain (Azevedo et al., 2015)	17°C	22°C
Sopron Hungary (Skarbit et al., 2017)	15°C	18.3°C
Kimmeria Greece (Papakostas et al., 2010)	15°C	24°C
Thessaloniki Greece (Papakostas et al., 2010)	15°C	24°C

Table 2. Base temperatures of each demo site location.

2.2.3 Current Trend calculations

The estimation of the current building energy needs is performed for the period November 2018 – October 2019, as for this timeframe the latest data are available. The maximum and minimum daily ambient temperatures were obtained from online databases (BizEE Software - Business Energy Efficiency Software, 2019). For each site the data of the nearest weather station are used.

2.2.4 Future Estimators of Building Load

The climate change and the associated temperature increase are expected to have a considerable impact on the energy demand globally. Europe will not be an exception, as it already experiences extreme weather conditions (heat and cold waves, draughts, floods etc.)(Spinoni et al., 2018), that are expected to intensify in the next decades. Therefore, in order to develop an integrated energy storage system that will be able to achieve considerable market penetration, it is necessary to estimate and consider not only the current but also the future energy demands that it will have to cover. In the framework of the current analysis, a short-term and a long-term future scenario are examined where the HDD and CDD for the years 2030 and 2050 are calculated respectively.

In order to perform the aforementioned estimations, the ASHRAE method is used again, along with the base temperatures depicted in Table 2. Future projections of daily mean air temperature have been obtained from Coordinated Regional Climate Downscaling Experiment (CORDEX) word climate research programme datasets regarding the two selected years (Horanyi, Copernicus). These datasets include the results of a significant number of simulations and their classification is based on the following criteria: a) the simulation resolution that can be either 0.44° (coarse) or 0.11° (fine), b) the used Regional Climate Model (RCM), c) the used Global Climate Model (GCM) that provides lateral and lower boundary conditions to RCM and d) the Representative Concentration Pathways (RCP) scenario utilized for producing boundary conditions regarding the concentrations of greenhouse gases in the atmosphere. There are four RCPs established in the fifth assessment report of Intergovernmental Panel on Climate Change (IPCC): RCP2.6, RCP4.5, RCP6.0 and RCP8.6 corresponding to an increase of radiative forcing of 2.6, 4.5, 6.0 and 8.6 W/m^2 by 2100 compared to the pre-industrial levels (van Vuuren et al., 2011). The related projections of CO_2 equivalent concentration are depicted in Figure 2.

In order to increase the accuracy of the daily mean temperature estimation for the years 2030 and 2050, the results of two different simulations were used. Both of them are bias-adjusted, i.e. they use as reference data for the period 1981-2010 the E-OBS high-resolution gridded dataset which results in the mitigation of inaccurate spatial patterns (Spinoni et al., 2018). The used climatic models are depicted in Table 3.

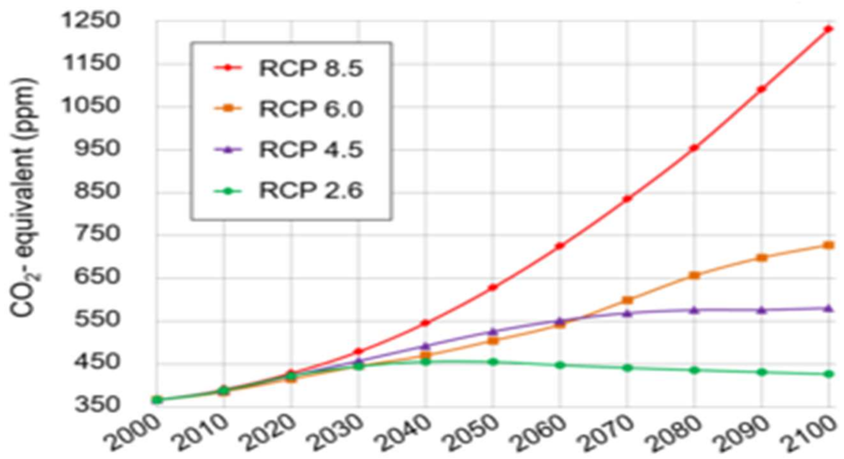

Figure 2: All forcing agents atmospheric CO2-equivalent concentrations (in ppm) according to the four RCP'S according to the IPCC AR5 report.(IPCC, 2014b)

GCM	RCM	GSM members	Resolution
HadGEM2-ES (UK Met Office, UK)	RCA4 (SMHI, Sweden)	r1i1p1	0.11°
IPSL-CM5A-MR (IPSL, France)	RCA4 (SMHI, Sweden)	r1i1p1	0.11°

Table 3. Characteristics of the used EURO-CORDEX simulations for future temperature estimations.

In both cases the selected RCP model is the moderate RCP4.5 according to which the equivalent CO_2 concentrations are expected to increase until 2080 reaching approximately 650ppm and then they stabilize in the period 2080 – 2100 (Thomson et al., 2011). The datasets of the first simulation provide estimations of the daily mean temperature for the period 1981 – 2098, whereas the second dataset extends to 2100. For each day of the selected years, i.e. of 2030 and 2050, the daily mean temperatures of the two simulations are averaged and the resulting temperature is used in order to calculate the HDD and CDD of that day according to equations 1 and 2. Moreover, in order to estimate the accuracy of this methodology, the current heating and cooling needs are also calculated by using the averaged simulation daily mean temperatures instead of the actual weather data. It is noted that the calculations for the Santiago site are done with the RCM LMD-LMDZ4NEMOMED8 (France) and a resolution of 0.44° due to data availability reasons, while the rest of the simulation characteristics remain the same.

2.2.5 Results of HDD/CDD calculations

The following charts and tables summarize the results of current (November 2018 – October 2019) and future (2030, 2050) estimations of annual building loads (HDD, CDD) for each demo site location. Figure 3 depicts the calculated annual sum of HDD and CDD for the period November 2018 – October 2018. As expected, HDD are significantly higher than CDD. Each demo site has different heat demands. Cork (Ireland) presents the highest annual heat demands of approximately 2800 HDD. The demo sites of Sopron in Hungary and Santiago in Spain have approximately 1970 and 1790 HDD respectively. As expected, the two Greek sites, Thessaloniki and Kimmeria, have the lower annual heating demands of approximately 1090 and 1150 HDD respectively. The cooling needs in Cork are almost zero. Also, the cooling loads are very small in Santiago. On the other hand, the calculated CDD are about 460 CDD for the demo site of Sopron. The resulted cooling needs in the two Greek sites are lower than those of Sopron. This is attributed to the fact that the base temperature for calculating the cooling demands in the latter case is 18°C, whereas in Greece the most suitable base temperature according to the literature is quite higher, namely 24°C (Papakostas et al., 2010). Furthermore, both sites are located in northern Greece and have a humid subtropical climate and a warm-summer Mediterranean climate respectively. Consequently, their calculated cooling demands are 355 CDD in the case of Thessaloniki and 270 CDD in the case of Kimmeria.

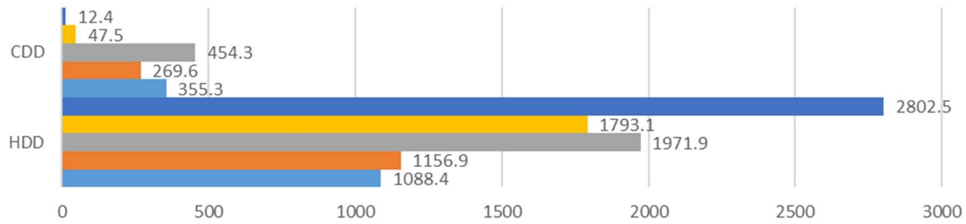

	HDD	CDD
Cork Ireland	2802.5	12.4
Santiago Spain	1793.1	47.5
Sopron Hungary	1971.9	454.3
Kimmeria Greece	1156.9	269.6
Thessaloniki Greece	1088.4	355.3

Figure 3: Current annual building loads (HDD, CDD) of each demo site location.

Table 4 presents the calculated current estimations of annual building loads by utilizing the average daily mean temperatures from the two simulations employed for the prediction of the energy demand in 2030 and 2050. It can be observed that in most cases the heating needs are calculated with very good accuracy and the corresponding relative error is lower than 8%. Regarding the CDD estimation, the results of weather data and simulation-based calculations are almost identical in the case of Thessaloniki. The same is also valid in the case of Cork, as regardless of the high relative error the absolute CDD values of the two methods are very close to each other. The cooling load of Kimmeria site is overestimated by approximately 23% when using simulation-based temperatures. On the contrary, CDD are considerably underestimated in the cases of Sopron and Santiago by 50% and 48.7% respectively. Noteworthy is the fact that the CDD values resulting from the temperatures of both simulation models share the same trend. In particular, the temperatures of HadGEM2-ES model lead to a CDD underestimation by 34.59% in the case of Sopron, compared to the CDD calculations based on weather data. Similarly, the temperatures of IPSL model result in lower CDD values by 69.19% for the Hungarian site and by 48.7% for the French one. To conclude, the current annual building loads estimations of Cork present the largest errors when using averaged simulation daily mean temperatures.

Location	HDD (simulation data)	HDD (relative error)	CDD (simulation data)	CDD (relative error)
Cork Ireland	3049.3	8.09%	8.6	-44.19%
Santiago Spain	1709	4.7%	24.4	-48.7%
Sopron Hungary	1989.5	0.88%	303.0	-49.93%
Kimmeria Greece	1210.2	4.40%	351.7	23.34%
Thessaloniki Greece	1117.4	2.60%	366.4	3.03%

Table 4. Current annual building loads (HDD, CDD) of each demo site location based on the averaged simulation daily mean temperatures and relative errors.

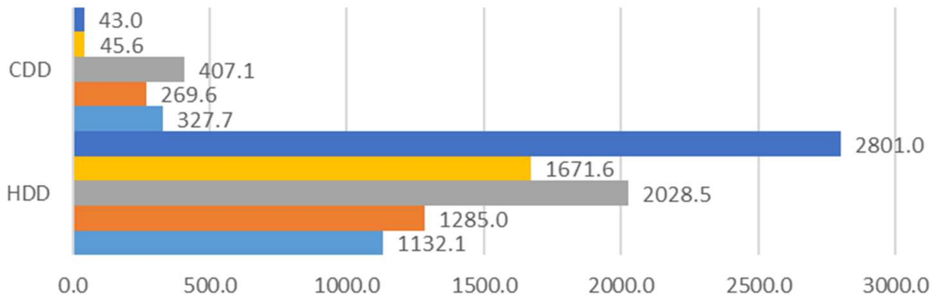

	HDD	CDD
Cork Ireland	2801.0	43.0
Santiago Spain	1671.6	45.6
Sopron Hungary	2028.5	407.1
Kimmeria Greece	1285.0	269.6
Thessaloniki Greece	1132.1	327.7

Cork Ireland · Santiago Spain · Sopron Hungary · Kimmeria Greece · Thessaloniki Greece

Figure 4. Annual building loads (HDD, CDD) in 2030 of each demo site location.

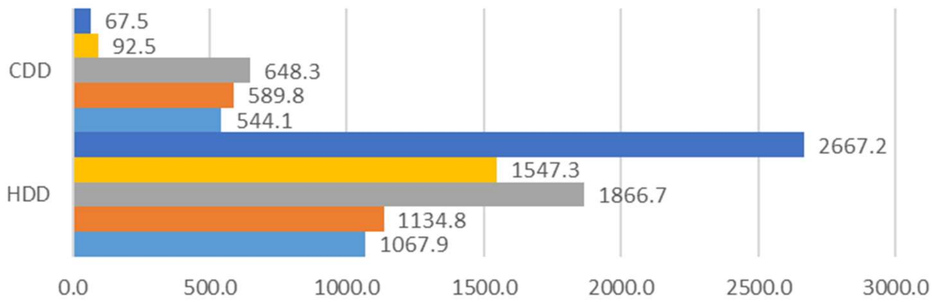

	HDD	CDD
Cork Ireland	2667.2	67.5
Santiago Spain	1547.3	92.5
Sopron Hungary	1866.7	648.3
Kimmeria Greece	1134.8	589.8
Thessaloniki Greece	1067.9	544.1

Cork Ireland · Santiago Spain · Sopron Hungary · Kimmeria Greece · Thessaloniki Greece

Figure 5. Annual building loads (HDD, CDD) in 2050 of each demo site location.

In Figure 4 and Figure 5, the future annual building loads for years 2030 and 2050 are presented respectively. The general trend is that the heating demands are increased in the short-term future scenario with the exception of Cork and Santiago, where they remain stable and reduced respectively. On the contrary the cooling demands variations do not present a uniform pattern. In particular, they increase in the case of Cork, they remain stable in the case of Kimmeria and Santiago but they are decreased in the cases of Sopron and Thessaloniki. Regarding the long-term future scenario, the estimations of the heating and cooling needs are more reasonable and in accordance with the conclusions of similar studies (Spinoni et al., 2018, Diffenbaugh et al., 2007, Isaac and Vuuren, 2009). The CDD values present an increase in almost all locations in comparison with the current needs, whereas the HDD values are decreased

In Figure 6 the percentage rate of change of HDD and CDD for each demo site location in respect to current weather data-based needs is presented. Cork experiences the highest increase of cooling demands (246% for the year 2030 and 444% for the year 2050), but this occurs since the current CDD are almost negligible. The value of CDDs is decreased for 2030 and forthe cases of Sopron, Santiago and Thessaloniki (-10%, -4.8% and -7.8% respectively). These sites share similar trends of CDD change also in 2050, as they are expected to increase by 42.7%, 94.8% and 53.1% respectively in comparison with current needs. In the case of Kimmeria the CDD values are expected to be more than double compared to 2018-9. Regarding HDD future estimations, in 2030 the heating needs are expected to increase especially in the cases of Kimmeria (11%). Sopron and Thessaloniki will experience a milder increase by 2.9% and 4% respectively, while the values of HDD are decreased in the Santiago case In 2050 Cork and Sopron present similar trends of HDD change, as in both cases they decrease by approximately 5% compared to 2018-9. Kimmeria and Thessaloniki also share the same decrease of heating needs by 1.9%. In the case of Santiago, the estimated HDD in 2050 are approximately 14% lower than the current ones.

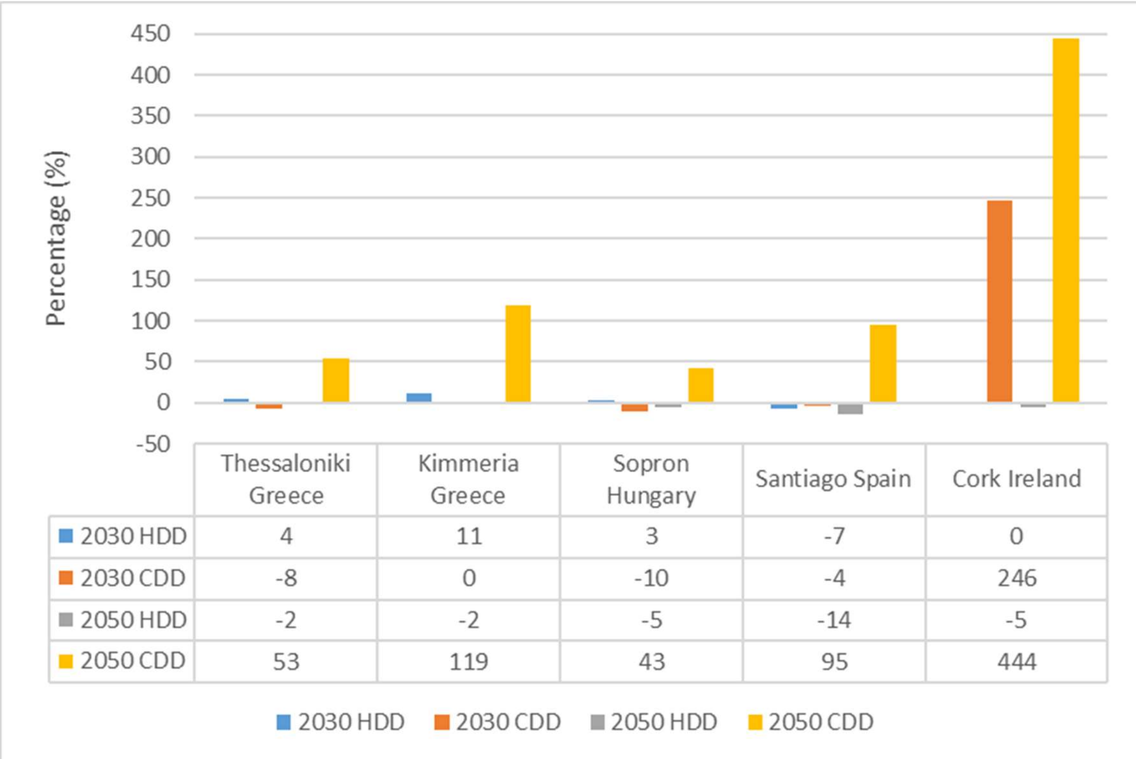

Figure 6. Relative change of HDD and CDD in respect to present amounts of degree days for each demo site location.

	Year	HDD	CDD	Mean HDD	Mean CDD	Peak HDD	Peak CDD
Cork Ireland	2018-9	2802.5	12.4	7.70	0.03	17.30	1.40
	2030	2800.9	42.9	7.73	0.12	17.67	3.76
	2050	2667.2	67.5	7.37	0.19	18.51	3.71
Santiago Spain	2018-9	1793.06	47.48	4.93	0.13	15.08	4.71
	2030	1671.63	45.58	4.59	0.12	11.96	3.95
	2050	1547.30	92.49	4.26	0.25	12.00	6.84
Sopron Hungary	2018-9	1971.9	454.3	5.42	1.24	20.30	8.60
	2030	2028.4	407.1	5.61	1.12	22.17	11.40
	2050	1866.7	648.3	5.16	1.79	19.24	12.18

Kimmeria Greece	2018-9	1156.9	269.6	3.19	0.73	17.10	5.80
	2030	1284.9	269.6	3.56	0.74	18.32	9.45
	2050	1134.8	589.8	3.14	1.62	16.86	11.14
Thessaloniki Greece	2018-9	1088.4	355.3	3.00	0.97	17.00	5.80
	2030	1132.1	327.7	3.13	0.90	14.90	9.09
	2050	1067.9	544.1	2.96	1.50	16.93	10.97

Table 5: Detailed summary results of degree-days of each demo site location.

Finally, in Table 5 a detailed summary of current and future degree-days for each demo site location is presented, including the values of annual mean daily HDD and CDD as well as the peak values within the examined year. As expected, mean values variation follows the same trend with the annual values variation, i.e. an increase of the latter results in an increase of the annual mean value. Peak HDD values also present a similar variation with the exception of Cork, where peak HDD values are expected to increase in the future even though the annual heating demands are expected to decrease. On the contrary, peak CDD values will increase in 2030 even in cases where the annual CDD load is stable or decreases as it happens in Sopron, Kimmeria and Thessaloniki. In Cork the CDD peak values will experience an increase in 2030 and seem to stabilize afterwards.In Santiago the peak CDD values are decreased in 2030, however they are increased in 2050. All the aforementioned future changes of peak heating and cooling needs denote that the tension of extreme weather conditions (cold and heat waves) is expected to increase in the future (Diffenbaugh et al., 2007).

In conclusion, our analysis shows a general decrease of future heating demands over Europe and an increase of future cooling needs, which is in agreement with the outcome of other studies (IPCC, 2014a). The examination of more than two unique years is necessary in order to define a more accurate and concrete pattern of the future heating and cooling needs in the five site locations, which is however out of the scope of the current analysis.

2.3 Definition of suitable estimators for thermal loads

Buildings are complex thermal environments that consist of a large number of variables that influence energy demand. The most accurate method for predicting energy consumptions is full dynamic thermal simulation. However, these calculations require a lot of input data to reach at reliable results and might also be time consuming (CIBSE, 2006). The proposed approach based on the degree-days concept, is a simplified method for energy estimation (heating and cooling) which requires only the knowledge of daily mean temperature and the annual energy usage of the building. Therefore, is suitable for performing current and future energy consumption estimations.

2.3.1 Method for estimating heating and cooling demand

There are many ways to illustrate the degree-day (DD) concept with respect to simplified heating analysis, as discussed by (Hitchin and Hyde, 1979). In all cases, the basic idea is that heating demand is a direct proportion of the indoor-to-outdoor temperature difference, such as (CIBSE, 2006):

$$Heat\ loss\ (kW) = overall\ heat\ loss\ coefficient\ (kW K^{-1}) \times temperature\ difference\ (K)$$

The overall heat loss coefficient is the combined representation of two coefficients that describe the building losses mechanism: a) the coefficient that is related to the losses due to the technical characteristics of the structure and is equivalent to the product of the heat exchanging area A with the overall heat transfer coefficient U, b) the coefficient that corresponds to the heat losses due to air infiltration. Equation 1 assumes steady state conditions and if these conditions prevail for a period of time, this expression will result in units of energy, i.e. kWh. As the outdoor air temperature varies, the temperature difference changes too, resulting in a proportional change in energy demand. In the case of ASHRAE method that was utilized in order to calculate the degree-days, the changes of temperature are considered to occur on daily basis (CIBSE, 2006). Therefore, the formula that provides the annual energy demand of a building is the following:

$$Energy\ demand\ \left(\frac{kWh}{year}\right) = overall\ heat\ loss\ coefficient\ (kWhK^{-1}) \times DD_{annual}\ (K/\text{year})$$

2.3.2 Results of thermal loads estimation

The following charts and tables summarize the results and calculations of current (November 2018 – October 2019) and future (2030, 2050) estimations of energy consumptions of the four demo sites. The four examined sites are: a) Cork (Ireland), Santiago (Spain), Sopron (Hungary), Kimmeria (Greece). Thessaloniki's pre-demo site will not be analyzed in this section due to the lack of information and data that are necessary in order to perform these estimations.

The Table below presents the current annual energy use and the corresponding degree-days of each examined building. Cork experiences the highest annual space heating usage (225 kWh/m²/year). This is expected due to the fact that the HDD are also the highest compared to other regions and because the construction year of the complex is 1966, with energy rating (BER) between D1 and C3. Furthermore, Santiago and Kimmeria have similar heating demands of 115.4 kWh/m²/year and 149 kWh/m²/year, respectively. Finally, Sopron's recent construction (2019-2020) combined with the fact that is a highly insulated building, result in the lowest heating demand per square meter (m²) of 23.16 kWh/m²/year. It should be remarked that the annual cooling demand in Cork and Santiago sites is not available. Kimmeria has a cooling demand of 29 kWh/year with a SEER (Seasonal Energy Efficiency Ratio) of 2.5, whereas in Sopron the cooling needs are almost negligible, 3kWh/m2/year, despite the fact that the annual CDD are 455.

	Construction year	Floor Area, m2	Space Heating, kWh/m²/year	Cooling, kWh/m²/year	Current HDD	Current CDD
Cork (Ireland)	1966	76	225	-	2802.5	12.4
Santiago (Spain)	1991	80.5	115.4	-	1793.1	47.5
Sopron (Hungary)	2019	187	23.16	3	1971.9	454.3
Kimmeria (Greece)	1997	150	149	29	1156.9	269.6

Table 6 Estimated energy consumption of each demo site

Table 7 depicts the calculated simplified overall heat loss coefficient of each demo site based on the data from Table 6 and the formula mentioned above. Kimmeria has the highest heat loss coefficient of 19.31 kWh/K followed by Cork with a coefficient of 6.1 kWh/K. The calculated coefficients of the below Table are combined with the current and future degree-days analysis can be helpful for performing an initial simplified dimensioning of the Ministor thermal energy system. The results of this analysis are presented for each demo site separately.

Overall Heat loss Coefficient, kWh/K		
Site	Heating	Cooling
Cork (Ireland)	6.1	-
Santiago (Spain)	0.24	-
Sopron (Hungary)	2.19	1.23
Kimmeria (Greece)	19.31	16.13

Table 7 Overall Heat loss coefficient of each demo site

This project has received funding from the European Union's Horizon 2020 research and innovation programme under grant agreement No 869821

The monthly thermal loads of Cork's (Ireland) site for current (2018-19), short-term (2030) and long-term future scenario (2050) is presented in Figure 7. Cork has the highest number of annual heating degree-days, approximately 2800. The highest monthly heating demand for 2018-19 occurs in January (2177.1 kWh). March is second in order with heating needs of 2027.6 kWh. Noteworthy is the fact that according to the HDD estimations, no month of the year is characterized by zero heating needs. However, the more intensive period lasts from October till May with demand ranging from 1347.9 up to 2177.1 kWh. The same pattern of heating needs distribution is also observed in the future projections. In year 2030, the energy demand from December till March is expected to be much higher than the current one, with the second highest value of 2469 kWh occurring in March. On the contrary, thermal loads in spring and summer months are significantly lower. In year 2050, the monthly thermal consumptions are estimated very close to the current ones, with the exception of the three summer months when they are considerably lower.

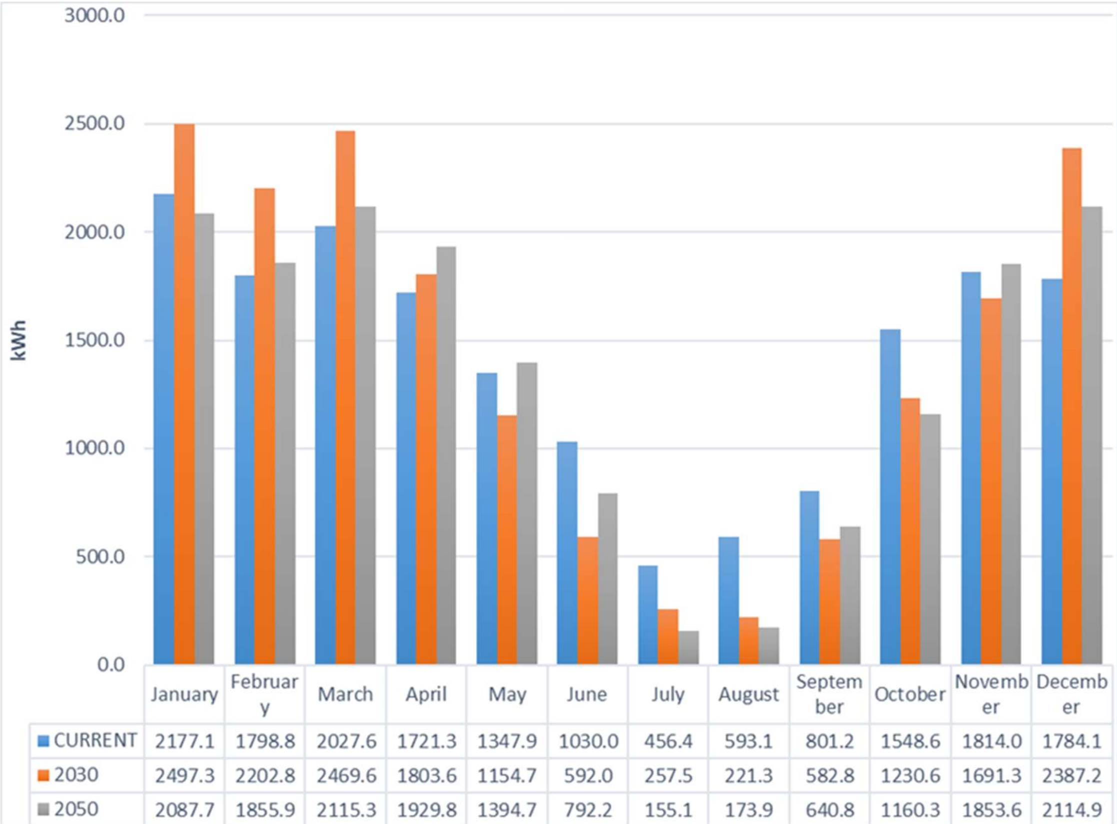

Figure 7 Monthly thermal loads in current year, 2030 and 2050 for Cork (Ireland) demo site

Cork (Ireland)	Daily Average Thermal Load (Current)	Daily Peak Thermal Load (Current)	Date of Peak Thermal Load (Current)	Daily Average Thermal Load (2030)	Daily Peak Thermal Load (2030)	Daily Average Thermal Load (2050)	Daily Peak Thermal Load (2050)
January	70.2	105.6	30-01-19	81.9	107.9	68.3	108.4
February	64.2	100.7	01-02-19	76.0	99.5	64.4	93.4
March	65.4	86.6	03-03-19	80.9	97.7	69.5	93.2
April	57.4	89.1	02-04-19	60.1	80.9	64.3	91.0
May	43.5	68.3	04-05-19	37.5	56.0	45.6	60.4
June	34.3	51.3	05-06-19	19.7	42.2	26.4	50.7
July	14.7	26.8	02-07-19	8.5	20.5	5.0	27.1

August	19.1	28.7	12/19-08-19	7.2	20.9	5.7	20.6
September	26.7	35.4	13-09-19	19.4	39.7	21.4	42.4
October	50.0	79.3	27-10-19	40.3	63.4	37.9	73.5
November	60.5	86.0	21-11-18	56.4	89.9	61.8	96.8
December	57.6	80.5	16-12-18	78.2	103.0	69.1	101.2

Table 8 Detailed summary of the daily average and peak thermal loads estimations (in kWh) for Cork (Ireland) demo site

In Table 8, a detailed summary of daily average and peak thermal load values for every month in the framework of the current scenario is presented, along with future estimations of these variables. Regarding daily average and peak thermal demand of 2018-19, the highest values are observed in January, 70.2 kWh and 105.6 kWh respectively. The day when the highest heating demand of the year occurs is the 30th January 2019. In the short-term future scenario, despite the fact that the total annual thermal loads are expected to increase, the daily average values seem to increase only in the period December – April. Similar also is the trend of the daily peak values. In year 2050, the daily average thermal loads tend to decrease in comparison with the current scenario especially in the cases of the summer months when loads as low as 5kWh are observed. December and April are the most notable exceptions to this trend. However, the daily peak values are increased in 2050 in five cases, with November and December presenting the more intense increment compared to 2018-9 and January exhibiting the highest daily thermal load of the year (108.4 kWh).

Figure 8 presents the current and future monthly heating demands in the case of Santiago del Compostela (Spain). In Santiago the heating demands are comparable to the other demo sites. The month that under current weather conditions presents the highest total heating demands of about 1.45 MWh is January. Similar to the Cork demo site, the Santiago demo needs space heating throughout the year, however during the summer period the corresponding demand drops significantly. According to the short-term future projections regarding 2030 (Fig. 8), the monthly heating demand decreases in most cases, however it increases in March reaching a high value of 1.36MWh (differing from the usual case nowadays which is January). Regarding the long-term future projections,the monthly thermal load during winter is in general lower than the present situation. However, notable is the fact that for the future forecasts, during the spring months and especially in April, the heating demands are expected to be higher than the current ones.

On both future scenarios, the heating demands of July and August are decreased compared to 2018-9 and especially in 2050 are expected to be almost zero. A similar analysis about the cooling demand of Santiago del Compostela demo site could not be performed since the annual calculated current CDD are small.

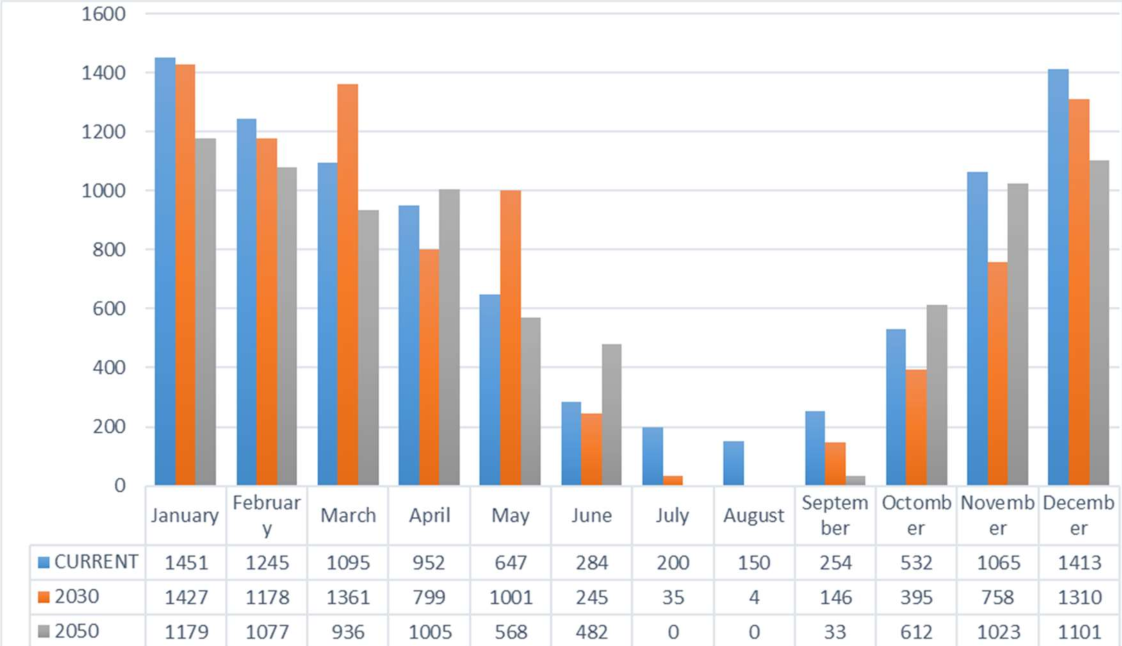

Figure 8 Monthly thermal loads in current year, 2030 and 2050 for Santiago (Spain) site

In Table 9, a detailed summary of daily average and peak values for every month of current period (2018-9), 2030 and 2050 are presented. Santiagos highest daily thermal load (78.1kWh) in 2018-19 is observed on 15th January 2019. There is also a similar heating demand of 273 kWh on 25th December 2018. These two months present also the highest daily average thermal needs of approximately 46kWh. In general, values of over 30 kWh per month are observed from November to April. Peak daily thermal loads in winter months tend to remain stable in both future scenarios. However, the corresponding values during autumn and spring are expected to increase in 2030, when May presents the highest daily heating demand of 61.9kWh. This value is almost 17% higher than corresponding thermal load of May 2019. The same pattern, although less intense is observed also in 2050, when the coldest day of the year occurs in December. The average daily thermal loads follow the same trend of milder winters and harsher autumns and springs in the future.

Santiago Spain	Thermal Load						
	Current			2030		2050	
	Daily Average	Daily Peak Thermal	Date of Peak	Daily Average	Daily Peak	Daily Average	Daily Peak
January	46.8	78.1	15/1/2019	46.0	61.4	38.0	53.5
February	44.5	72.1	15/2/2019	42.1	58.5	38.5	55.5
March	35.3	61.7	8/3/2019	43.9	61.9	30.2	45.1
April	31.7	56.9	30/4/2019	26.6	52.9	33.5	57.2
May	20.9	41.5	12/5/2019	32.3	48.5	18.3	51.1
June	9.5	22.3	-	8.2	33.6	16.1	36.9
July	6.4	18.2	-	1.1	8.3	0.0	0.0
August	4.8	14.2	-	0.1	3.7	0.0	0.0
September	8.5	19.7	28/9/2019	4.9	24.7	1.1	12.9
October	17.2	37.8	28/10/2019	12.7	36.2	19.7	52.2
November	35.5	61.9	29/11/2018	25.3	53.3	34.1	55.2
December	45.6	76.5	25/12/2018	42.2	57.7	35.5	62.2

Table 9 Detailed summary of daily average and peak thermal loads estimations (in kWh) for Santiago (Spain) site

Figure 9 and Figure 10 display the monthly thermal and cooling loads of current year (2018-9), 2030 and 2050 for Sopron demo site (Hungary). This construction meets the requirements of Nearly-Zero Energy Building (nZEB), so it is expected to have low thermal and cooling energy consumptions. It has to be mentioned here that the current CDD based on simulation temperatures are considerably underestimated by 50%, in contrary to the accurate HDD estimations of which the relative error is 0.88%. In the current case, the month with the highest heating demand of about 980kWh is January 2019. Contrary to Santiago and Cork demos, Sopron demo does not require space heating during the summer months. It can be assessed that the intensive heating period lasts from November till March with loads ranging from 430 up to 980.9 kWh. Regarding the short-term future projections for the space heating, a slight decrease from September until January is observed accompanied by significant increase from February until April. Consequently, the annual heating needs which remain more or less stable between 2018-9 and 2030, present different distribution patterns. The long-term future scenario presents a similar trend of monthly heating demand needs with 2018-9. The most notable exceptions are observed in January and September, when the monthly thermal load decreases, whereas in March and April the corresponding values increase.

Cooling demand for the current year is needed mainly from June until September and the highest monthly load of 176.1kWh occurs in June. It can be observed that the monthly cooling needs, experience a moderate decrease in 2030 and a moderate increase in 2050 compared to the current case. In both future scenarios the highest monthly cooling load is observed in July, when values of 208.4kWh in 2030 and 307.8kWh in 2050 are estimated respectively. In conclusion, estimated thermal and cooling demands of this demo site are rather low considering the relevant large floor area (187m²).

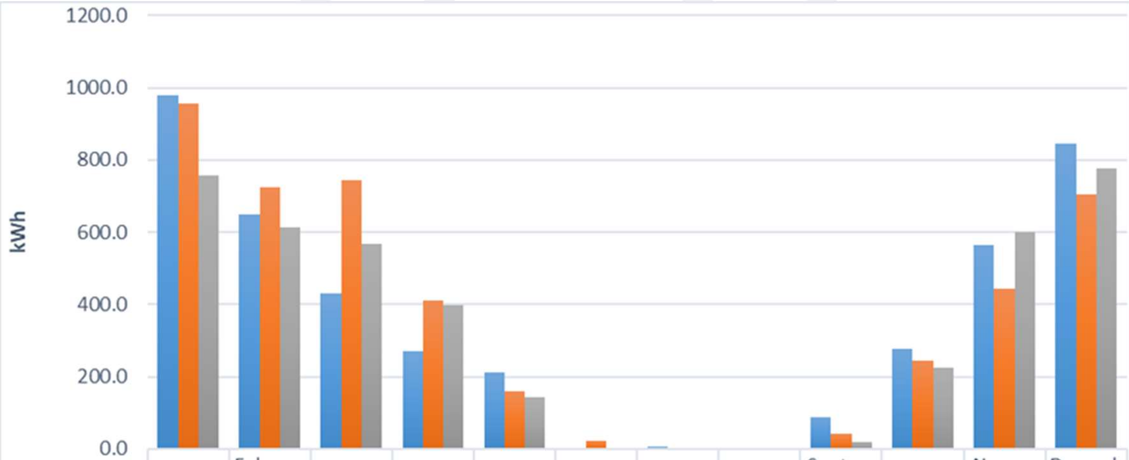

	January	February	March	April	May	June	July	August	September	October	November	December
CURRENT	980.9	650.1	430.0	272.1	213.0	1.5	5.5	3.5	87.0	275.9	565.1	846.2
2030	956.8	723.3	743.9	409.9	161.1	23.7	0.0	0.0	43.1	244.2	442.7	706.4
2050	758.2	614.9	567.1	397.6	144.4	0.0	0.0	0.0	18.0	225.1	599.1	775.6

Figure 9 Monthly thermal loads in current year, 2030 and 2050 for Sopron (Hungary) site

This project has received funding from the European Union's Horizon 2020 research and innovation programme under grant agreement No 869821

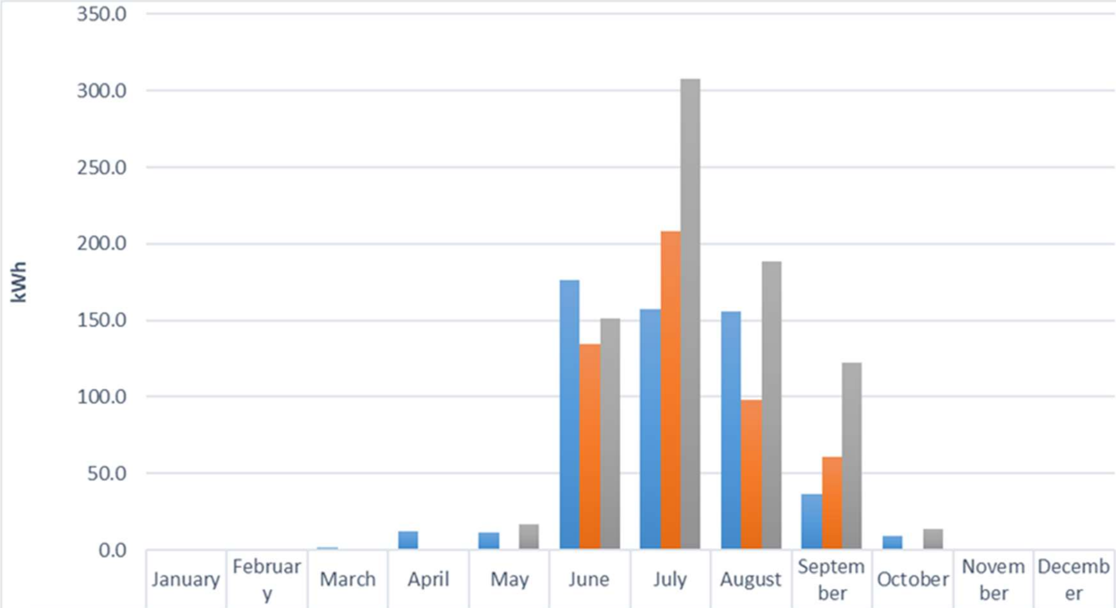

	January	February	March	April	May	June	July	August	September	October	November	December
CURRENT	0.0	0.5	1.4	12.3	11.4	176.1	157.3	156.0	36.6	9.5	0.0	0.0
2030	0.0	0.0	0.0	0.0	0.4	134.7	208.4	98.4	60.5	0.3	0.0	0.0
2050	0.0	0.0	0.0	0.0	17.1	151.1	307.8	188.7	122.0	13.8	0.0	0.0

Figure 10 Monthly cooling loads in current year, 2030 and 2050 for Sopron (Hungary) site

The two Tables below present a detailed summary of the daily average and peak thermal and cooling loads for Sopron demo site. In Table 10, the current energy consumption is depicted and in Table 11 are the future projections. The demo site current highest daily heating demand is 44.6 kWh and occurs on 22nd January 2019. The same month presents also the highest daily average heating needs of 31.6kWh. The highest daily cooling demand of 10.6 kWh is observed on 26th June 2019.

Regarding future projections depicted in Table 11, it can be observed that peak daily cooling load values will increase over the years, especially in July and September. In both future scenarios the highest values are observed in July, when values of 13.2kWh in 2030 and 15kWh in 2050 are estimated respectively. Daily average cooling load follows the same pattern with daily peak values. July is the month that presents the highest average cooling needs of 6.9kWh in 2030 and 10.1kWh in 2050 respectively, the latter value is almost doubled compared to the current case. Peak thermal loads are increasing in the period January-April and decreasing in the rest of the year in 2030 with the highest value of 48.7kWh observed in January 2030. On the contrary they experience a general decrease in 2050 compared to current case, with the exception of March, April and December.

In the latter case the highest daily thermal needs of 41.9kWh occur. The future projections of daily average heating needs present the same pattern with the overall monthly needs in 2030, i.e. they decrease from September until January and increase from February until April. In 2050, the most notable differences compared to the present year are the higher average daily values in March and April. Overall, the thermal consumptions of Sopron (Hungary) are expected to remain stable in the future. This is closely related to the HDD analysis, according to which the percentage rate of change of this variable is 2.9% and -5.3% for 2030 and 2050 respectively. On the other hand, cooling consumptions of this demo site tend to increase and become more intense.

Sopron (Hungary)	Daily Average Thermal Load (2018-9)	Daily Peak Thermal Load (2018-9)	Date of Peak Thermal Load (2018-9)	Daily Average Cooling Load (2018-9)	Daily Peak Cooling Load (2018-9)	Date of Peak Cooling Load (2018-9)
January	31.6	44.6	22-01-19	0.0	0.0	-

February	23.2	36.9	23-02-19	0.0	0.5	28-02-19
March	13.9	22.0	20-03-19	0.0	0.5	17-03-19
April	9.1	17.6	14-04-19	0.4	4.1	25-04-19
May	6.9	20.9	05-05-19	0.4	2.6	26-05-19
June	0.1	0.9	30-06-19	5.9	10.6	26-06-19
July	0.2	1.5	11-07-19	5.1	9.8	26-07-19
August	0.1	1.8	17-08-19	5.0	8.9	10-08-19
September	2.9	11.2	21-09-19	1.2	5.6	01-09-19
October	8.9	26.1	31-10-19	0.3	1.9	01-10-19
November	18.8	40.0	29-11-18	0.0	0.0	-
December	27.3	38.9	17-02-18	0.0	0.0	-

Table 10 Detailed summary of daily average and peak thermal and cooling loads estimations (in kWh) for Sopron (Hungary) site

Sopron (Hungary)	Daily Average Thermal Load (2030)	Daily Peak Thermal Load (2030)	Daily Average Cooling Load (2030)	Daily Peak Cooling Load (2030)	Daily Average Thermal Load (2050)	Daily Peak Thermal Load (2050)	Daily Average Cooling Load (2050)	Daily Peak Cooling Load (2050)
January	31.3	48.7	0.0	0.0	24.9	41.1	0.0	0.0
February	25.0	39.0	0.0	0.0	21.1	34.4	0.0	0.0
March	24.3	32.2	0.0	0.0	18.7	29.6	0.0	0.0
April	13.7	25.8	0.0	0.0	13.3	23.3	0.0	0.0
May	5.3	13.6	0.0	0.4	4.7	15.5	0.6	3.4
June	0.8	3.6	4.5	11.2	0.0	0.0	5.0	11.4
July	0.0	0.0	6.9	13.2	0.0	0.0	10.1	15.0
August	0.0	0.0	3.2	8.9	0.0	0.0	6.2	12.4
September	1.4	8.7	2.0	9.2	0.6	3.8	4.1	10.8
October	8.0	16.9	0.0	0.3	7.4	21.5	0.4	3.5
November	14.8	30.0	0.0	0.0	20.0	33.8	0.0	0.0
December	23.2	35.8	0.0	0.0	25.5	41.9	0.0	0.0

Table 11 Detailed summary of future daily average and peak thermal and cooling loads estimations (in kWh) for Sopron (Hungary)

Figure 11 and Figure 12 present the monthly thermal and cooling loads in all three examined scenarios (2018-9, 2030 and 2050) for Kimmeria (Greece) site. Kimmeria's site has the second highest heat demand compared to the other demo sites, because of its 150 m2 floor area. As expected, this building experiences the hottest summers due to its location and as a result it has the highest cooling demand. Kimmeria, just like the Sopron site, presents distinct heating and cooling periods. The heating period lasts from November until April and the cooling one from June till September. The peak monthly value for space heating in 2018-9 is 5708.7 kWh and occurs in January 2019. In short-term future estimations there is an increase of heating loads from January until April, especially in March it is close to 55%. This trend is less intense in long-term future projections and significant increase compared to the current case is spotted only in January and February. In both future cases, December is expected to be milder than that of the year 2018 and January is the harshest month of the year with monthly thermal loads of 6270.6kWh in 2030 and 6025.4kWh in 2050.

Regarding monthly cooling needs, the peak value of 1649 kWh occurs in August 2019. In 2030, the annual cooling load is the same with the base year 2018-9, but monthly load experiences a considerable decrease in June and a significant increase in July. On the contrary, in 2050, the annual cooling consumption is increased by 53% compared to the current case, in accordance with the CDD analysis. This difference is reflected in the monthly load of all months and particularly in the cases of July and August, when values higher than 3400kWh are observed.

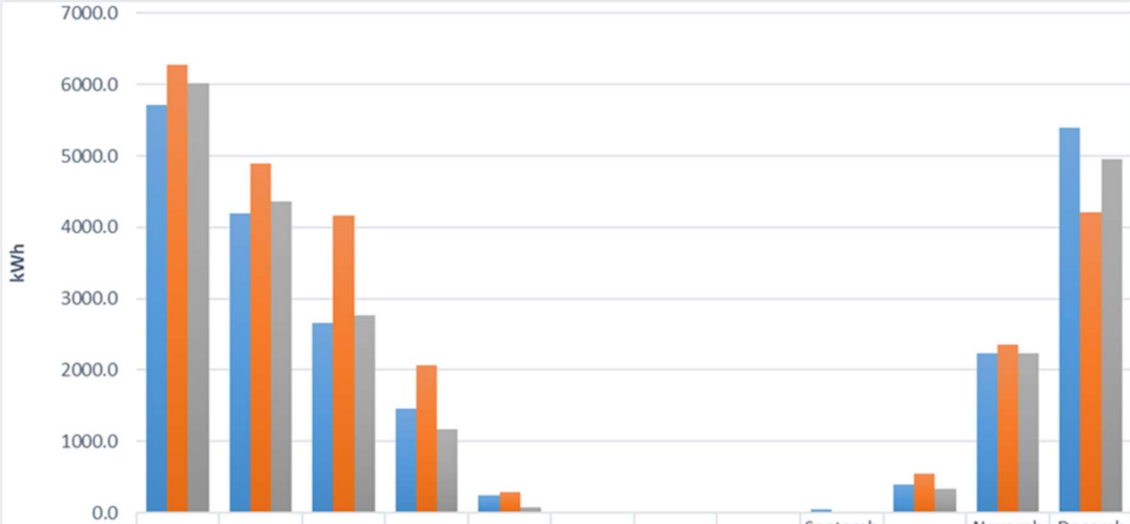

	January	February	March	April	May	June	July	August	September	October	November	December
CURRENT	5708.7	4201.9	2667.9	1452.8	241.5	1.9	0.0	0.0	48.3	392.2	2239.1	5395.8
2030	6270.6	4900.6	4157.9	2070.7	295.0	0.0	0.0	0.0	0.0	553.9	2361.3	4213.9
2050	6025.4	4369.0	2761.3	1169.8	83.0	0.0	0.0	0.0	0.0	328.8	2232.6	4953.8

Figure 11 Monthly thermal loads in current year, 2030 and 2050 for Kimmeria (Greece) site

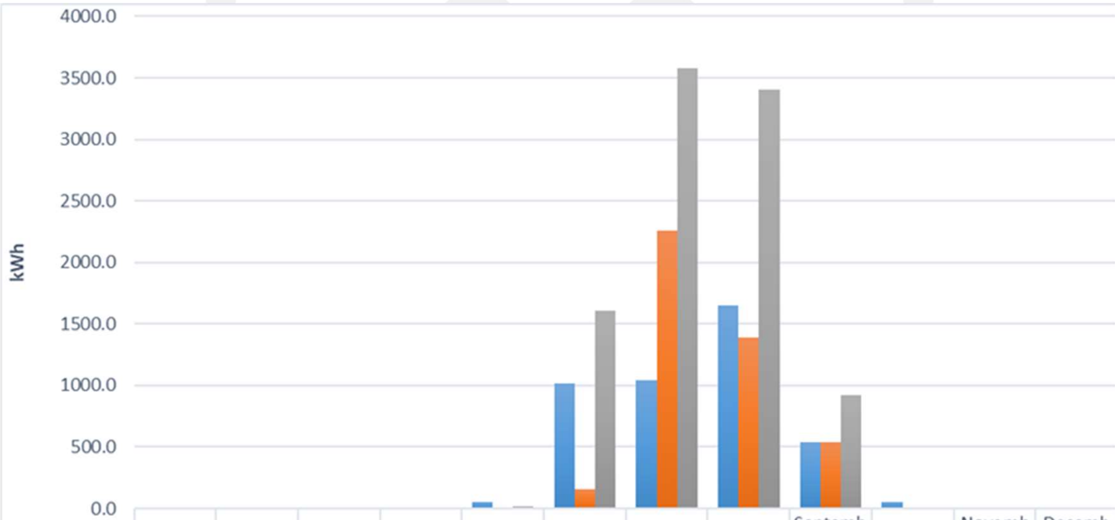

	January	February	March	April	May	June	July	August	September	October	November	December
CURRENT	0.0	0.0	0.0	0.0	54.9	1016.5	1040.7	1649.0	540.5	48.4	0.0	0.0
2030	0.0	0.0	0.0	0.0	0.0	160.4	2256.1	1392.4	541.1	0.0	0.0	0.0
2050	0.0	0.0	0.0	0.0	16.9	1603.6	3576.7	3402.4	917.5	0.0	0.0	0.0

Figure 12 Monthly cooling loads in current year, 2030 and 2050 for Kimmeria (Greece) site

Kimmeria (Greece)	Daily Average Thermal Load (2018-9)	Daily Peak Thermal Load (2018-9)	Date of Peak Thermal Load (2018-9)	Daily Average Cooling Load (2018-9)	Daily Peak Cooling Load (2018-9)	Date of Peak Cooling Load (2018-9)
January	184.2	330.4	08-01-19	0.0	0.0	-
February	150.1	272.4	24-02-19	0.0	0.0	-
March	86.1	148.8	14-03-19	0.0	0.0	-
April	48.4	102.4	04-04-19	0.0	0.0	-
May	7.8	42.5	09-05-19	1.8	14.5	30-05-19
June	0.1	1.9	03-06-19	33.9	79.1	25-06-19
July	0.0	0.0	-	33.6	66.2	04-07-19
August	0.0	0.0	-	53.2	93.6	25-08-19
September	1.6	19.3	21-09-19	18.0	53.2	04-09-19
October	12.7	38.6	28-10-19	1.6	22.6	01-10-19
November	74.6	202.8	30-11-18	0.0	0.0	-
December	174.1	243.4	26-12-18	0.0	0.0	-

Table 12 Detailed summary of daily average and peak thermal and cooling loads estimations (in kWh) for Kimmeria (Greece) site

The above Table displays the current daily average and peak thermal and cooling loads. Kimmeria's highest daily heating demand is 330.4 kWh and is observed on 8th January 2019. The same month presents also the highest daily average heating needs of 184.2kWh, whereas December 2018 is also a month with significant loads of 174.1kWh. On the contrary, the highest daily cooling demand of 93.6 kWh is observed on 25th August 2019. The most intense daily average cooling needs are also spotted in this month.

The Table below presents the future projections of daily average and peak thermal and cooling needs. Peak daily cooling loads are expected to decrease in June and increase from July until September. Especially in July 2030 the peak daily demand is almost double compared to July 2019. In 2050, the peak daily needs of all months are expected to increase and both July and August experience values of over 170kWh. Daily average cooling load follows the same pattern with daily peak values. July is the month that presents the highest average cooling needs of 74.6kWh in 2030 and 117.5kWh in 2050 respectively, the latter value is more than tripled compared to the current case. In the long-term future scenario August presents also significant average cooling loads of 111.5kWh. These assessments might be moderate if we take into account the fact that current CDD are underestimated by 23.34% when using simulation-based temperatures. Peak thermal loads are increasing in the spring months as well as in October of 2030, with the highest value of 353.9kWh observed in January of that year. On the contrary, only March and October experience a more moderate increase in 2050 compared to current case. Again, January is the month when the most intense daily heating demands of 325.6kWh occur.

Average space heating loads are expected to increase in 2030 throughout the heating period with the exception of December. In 2050 an opposite trend is expected to prevail. The average daily needs will be decreasing in all cases and only in January and March experience a small increase compared to the present year.

Kimmeria (Greece)	Daily Average Thermal Load (2030)	Daily Peak Thermal Load (2030)	Daily Average Cooling Load (2030)	Daily Peak Cooling Load (2030)	Daily Average Thermal Load (2050)	Daily Peak Thermal Load (2050)	Daily Average Cooling Load (2050)	Daily Peak Cooling Load (2050)
January	205.5	353.9	0.0	0.0	197.5	325.6	0.0	0.0
February	169.6	248.2	0.0	0.0	149.7	237.7	0.0	0.0

March	135.7	225.3	0.0	0.0	90.7	208.6	0.0	0.0
April	69.0	143.7	0.0	0.0	39.0	111.8	0.0	0.0
May	9.7	74.5	0.0	0.0	2.7	34.3	0.6	14.9
June	0.0	0.0	5.3	35.5	0.0	0.0	53.5	91.0
July	0.0	0.0	74.6	136.6	0.0	0.0	117.5	172.2
August	0.0	0.0	45.6	124.8	0.0	0.0	111.5	179.2
September	0.0	0.0	18.0	61.7	0.0	0.0	30.6	91.4
October	18.2	87.2	0.0	0.0	10.8	72.8	0.0	0.0
November	78.7	174.5	0.0	0.0	74.4	187.4	0.0	0.0
December	138.1	243.5	0.0	0.0	163.0	254.0	0.0	0.0

Table 13 Detailed summary of future daily average and peak thermal and cooling loads estimations (in kWh) for Kimmeria (Greece)

The purpose of the current analysis is to estimate the thermal and cooling loads in each demo site, that the novel integrated energy storage system will have to cover. Consequently, the outcome of this study will be used as an input for the system initial dimensioning. Table 14 summarizes the basic energy requirements that MiniStor system should meet, i.e. the daily average and peak load calculated in an annual basis for all three scenarios (2018-9, 2030 and 2050). In the estimation of the daily average thermal and cooling needs only the months with significant thermal and cooling loads respectively have been taken into account. In particular the daily average thermal load is calculated throughout the year excluding July and August in the cases of Cork and Santiago, excluding the three summer months in the case of Sopron and excluding the period May – September in the case of Kimmeria. The daily average cooling load is computed taking into account the demand of the period from June to September in all cases, with the exception of short-term scenario in Kimmeria in which June is excluded.

Period	Daily Average Thermal Demand (kWh)	Daily Peak Thermal Demand (kWh)	Daily Average Cooling Demand (kWh)	Daily Peak Cooling Demand (kWh)
Cork (Ireland)				
2018-19	53.0	105.6	-	-
2030	55.0	107.9	-	-
2050	52.9	108.4	-	-
Santiago (Spain)				
2018-19	29.5	78.1	-	-
2030	28.4	61.9	-	-
2050	26.5	62.2	-	-
Sopron (Hungary)				
2018-19	17.4	44.6	4.3	10.6
2030	18.1	48.7	4.1	13.2
2050	16.9	41.9	6.3	15.0
Kimmeria (Greece)				
2018-19	104.2	330.4	34.7	93.6
2030	116.3	353.9	46.1	136.6
2050	103.5	325.6	78.2	179.2

Table 14 Detailed summary of daily average and peak thermal and cooling loads estimations for each demo site

In each demo site, the installed system should be able to cover the current average loads and a percentage of the current peak loads, provided that the solar resources allow for this. The future average heating needs do not differ significantly from the current ones. On the contrary, the peak thermal loads present in some cases considerable differences, with the highest one of 353.9kWh being spotted in the case of Kimmeria. Kimmeria demo site is expected to experience significant increase of the daily average cooling loads in the future. Almost the same is the trend of the daily peak cooling demand which is projected to almost double in 2050. In order to take these future variations into account, a modular design of MiniStor will be adopted. More particularly, the TCM reactor will consist of several tubes, containing reactive material and connected in such a way that corresponds to the desirable energy storage capacity. The number of these tubes can be easily increased or decreased, resulting in an adaptation of the overall heating and cooling capacity of the system to the required heating and cooling demand.

Regarding the balance between heat and cold storage, MiniStor design is expected to achieve a ratio of 2.1:1 (i.e. a system with a 17.5 kWh TCM reactor can produce around 17.5 kWh of heat and 8.8 kWh of cold). This ratio is in most cases lower than the ratios of future heating to cooling needs resulting from Table 14. Nevertheless, the system cooling output could be further enhanced by exploiting the current ammonia cycle and operating it as a conventional refrigeration cycle, bypassing the TCM reactor. This modification could be conceptually explored during the design phase of the system, but its implementation in the prototypes would be avoided to keep their degree of complexity as low as possible. However, it could be realized in a more mature system design stage. In combination with the aforementioned possible modifications, the capacity of the PCMs (both cooling and heating) can be increased in order to be able to store higher amounts of energy. Finally, the data of Table 14 could be combined with more accurate calculations of current heating and cooling needs based on more detailed information of the demo site configuration, in order to define the system characteristics in each case. More details about the system design can be found in the corresponding deliverables of WPs 3 and 4.

2.4 Regional characterization through heating and cooling demand

The MiniStor heat storage system can be an asset to help in the wider implementation of renewable energy networks, by increasing the availability of heat generated from solar energy. Heating and cooling demand for human activities can also be studied at the regional level. Such studies can be done through geographical information systems (GIS), in order to identify energy scenarios according to available resources.

An example of such categorization can be found in the HOTMAPS project database (Hotmaps Project, 2019) which shows data for the EU 28 to the district and sometimes the property level. The code and data is open source, and provides information on a series of data such as total building volume for the selected region, floor area, estimated emissions, etc. This information is overlaid graphically on a map of Europe that can be augmented according to the desired level of analysis (which also depends on the level of information available). The database also provides a heatload profile for the region in terms of maximum, minimum and average demand. These have been obtained from benchmark calculations according to predominant activities in the region, deriving indicators for potential use. Although in some cases analysis in this tool can be made down to the size of several urban blocks, caution must be made due to the size of the regional sampling units used for some countries. Such regional divisions define how much built area is included and the activities performed in it. Therefore, geographical comparisons between regions can only be made if they have similar size or activity level.

Data shown is in general agreement with the location being studied, with countries located on Northern areas having higher heat power demand than those on the Southern countries. An example follows for Paris, France:

This project has received funding from the European Union's Horizon 2020 research and innovation programme under grant agreement No 869821

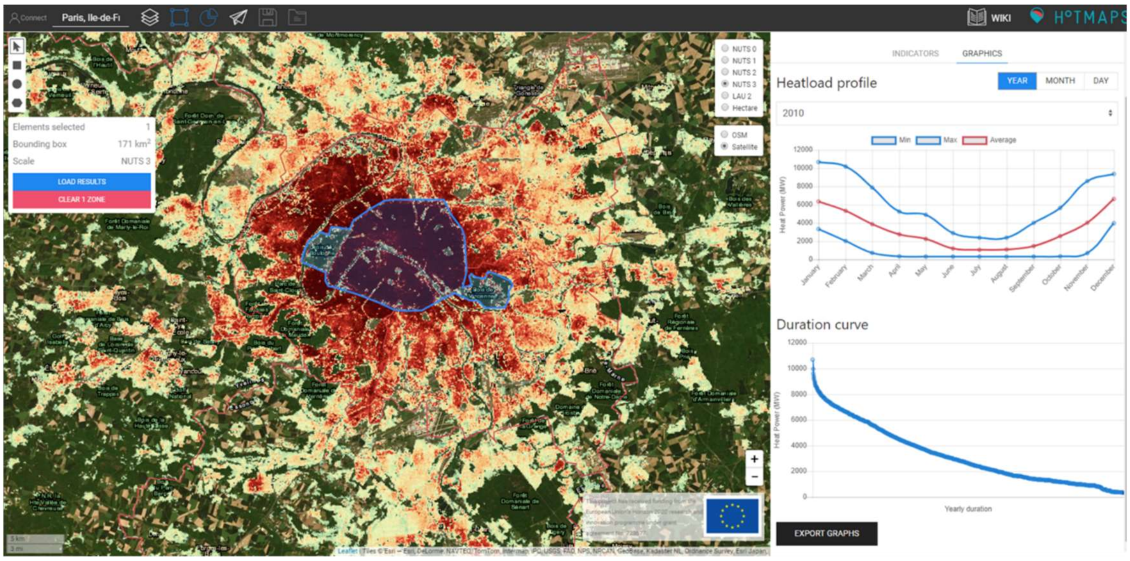

Figure 13 Sample HOTMAPS heatload profile for the Paris urban area. Source: https://www.hotmaps.hevs.ch/map

2.5 Solar energy availability databases for Europe

The proposed MiniStor system configuration will use solar energy as the renewable source from which it will store heat and generate electrical power. Therefore, it is important to have an overview of solar energy availability for a given location that can affect possible energy outputs and storage capabilities.

In order to quantify this availability, there are different databases that offer solar radiation data for particular cities, regions and for the entire world. These databases usually require post-processing in order to provide complete information to calculate and simulate solar energy facilities.

The most common data sources that offer post-processed solar radiation information at European level are Meteonorm and PVGIS. On a global level, the weather database available at the EnergyPlus weather website is also commonly used, but it is limited to the locations contained in the database.

The main characteristics of the data sources mentioned are briefly explained below, with the corresponding links indicated in the References section:

2.5.1 Meteonorm

Meteonorm is a software application for use in computer systems developed by Meteotest (Meteonorm, 2020). It uses as its main raw source monthly meteorological data from standardized ground meteorological stations located around the world, and satellite observations for radiation interpolation in remote regions where no radiation measurement is carried out on the ground. Such data is interpolated to obtain hourly synthetic solar radiation data that covers an entire year. Using a similar method, Meteonorm is able to use interpolation algorithms in order to obtain the climatic and solar radiation data of sites located at intermediate points between meteorological stations. The presence of several meteorological stations in a given area decreases the uncertainty level of its data. Specific data sets are available according to specific years, in addition to abstracted representative data such as the Typical Meteorological Year (TMY).

This project has received funding from the European Union's Horizon 2020 research and innovation programme under grant agreement No 869821

Since the source data for this database is based mainly on standardized meteorological stations, its accuracy is considered to be high. Therefore, it is widely used for studies and simulations at research level and also in different commercial programs. However, it does not take into account the shading effect of mountains at sunrises and sunsets, which must be accounted for when designing in mountain regions (PVSyst, 2019).

A caveat is that the use of Meteonorm is subject to a license and payment. Data sets are available as stand-alone products which are also available after payment. One of these products is the "solar cadastre", where solar resources on rooftops are readily calculated. However, some simulation software, such as TRNSYS and POLYSUN, already provide weather data (including solar radiation) from Meteonorm, for different European locations.

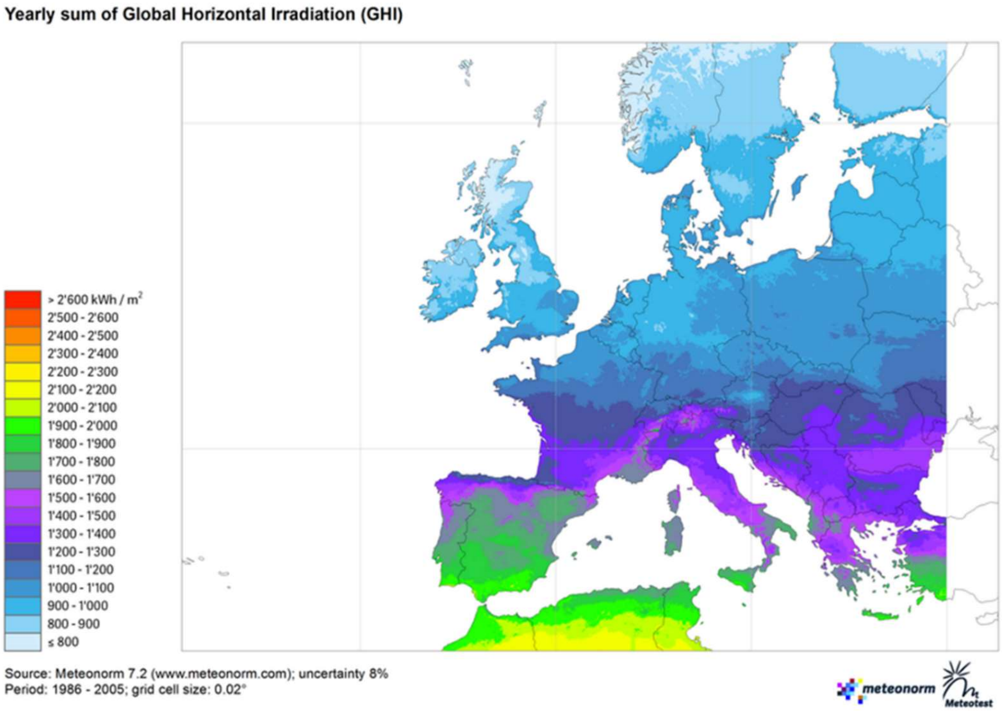

Figure 14 Global Horizontal Irradiation map for Europe. Source: Meteonorm

2.5.2 PVGIS

The Photovoltaic Geographical Information System (PVGIS) is a freely available, web-based application developed by the Joint Research Centre (JRC) of the European Commission (PVGIS, 2020). Its objective is to facilitate the initial calculation of photovoltaic solar installations in Europe and large areas worldwide (about 80% of the inhabited land masses).

The main data source for this application and database consists primarily of high-resolution geostationary meteorological satellite data with corrective algorithms. It also uses recalculated weather forecast models with corrections based on measured ground observations. Data obtained from ground meteorological stations has more accuracy but lower resolution. Satellite data has less accuracy, but it is possible to have a higher resolution, by using advanced algorithms to interpolate missing data or account for factors such as cloud cover. The quality and accuracy of information obtained from satellites has improved greatly during the last decade.

An advantage of PVGIS is that it allows the free download of geographical information system (GIS) and spreadsheet data for use in solar calculations and representation in maps. The spreadsheet version contains detailed data for EU and other European countries regarding solar radiation and PV potential summary for fixed-mounted PV systems. In addition, PVGIS also offers tools that provide to obtain monthly, daily and hourly series of solar radiation, as well as TMY files and horizon profiles.

Using a general overview, and when applied to the urban areas of the demonstration sites, PVGIS provides the following preliminary results, which will be subject to change and further study, as shown in the following figure:

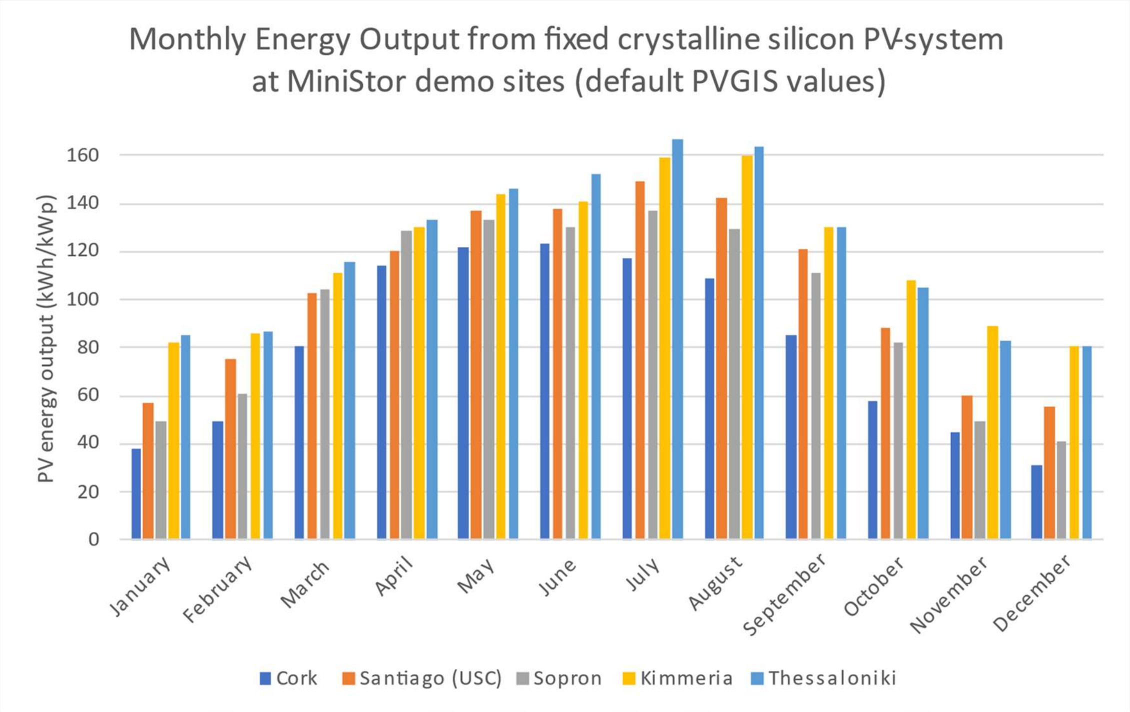

Figure 15 Monthly energy output from a theoretical, grid-connected fixed PV system for the demonstration sites. Source: PVGIS

Default values were used, as presented in the web-based tool. The results show the expected geographical variation between PV systems located in Northern and Southern European countries, and that there are high possibilities in each of them for using renewable energy. Although there is a marked difference between North and South in terms of overall solar radiation during the year, electrical outputs using conventional PV technologies still offer high possibilities continent-wide for their use.

2.5.3 EnergyPlus – Weather Data

EnergyPlus is a software created by the Building Technologies Office (BTO) of the U.S. Department of Energy (DOE). It is managed by the National Renewable Energy Laboratory (NREL) (U.S. Department of Energy, 2020). The main purpose of this software is for whole-building energy analysis through modelling. However, to produce results it requires detailed meteorological data from very close time intervals. When it was originally released, few energy simulation programs had such requirements, therefore its own file format was developed for weather files. Both the software and the associated weather files are freely available for download through the EnergyPlus website.

There, users can find weather data files (Including solar radiation) for several locations around the world, with many more locations being added. Information in the files is based mainly on International Weather for Energy Calculations (IWEC) databases and other local databases from different countries. The file would contain, among others, data on: temperature, humidity, extraterrestrial and global radiation, illuminance, sky cover, etc., covering the entire year. For locations that are not included in the weather data repository, there is the possibility to produce a "synthetic" weather file based on observations from nearby meteorological stations, calculated solar radiation, etc. Some of these files are offered by companies specialized in producing such type of data. Thus, it can be possible to use this data even for other locations such as some of the demo sites.

Usually the files available represent a typical meteorological year (TMY) for the location, since EnergyPlus can also be used for component sizing in buildings, such as HVAC systems. Therefore, the assumptions used to formulate those files must be taken into account, such as that a TMY file is based on what is thought to be the "average" of long-term observations in a given historical period with certain extremes not being taken into account. EnergyPlus has other file formats that take into account extreme conditions that would be useful for HVAC equipment sizing.

Nevertheless, the use of weather files in EnergyPlus format (EPW) is widespread and has been adopted as a type of standard in the energy modelling community. For example, they can be used in other simulation programs such as TRNSYS.

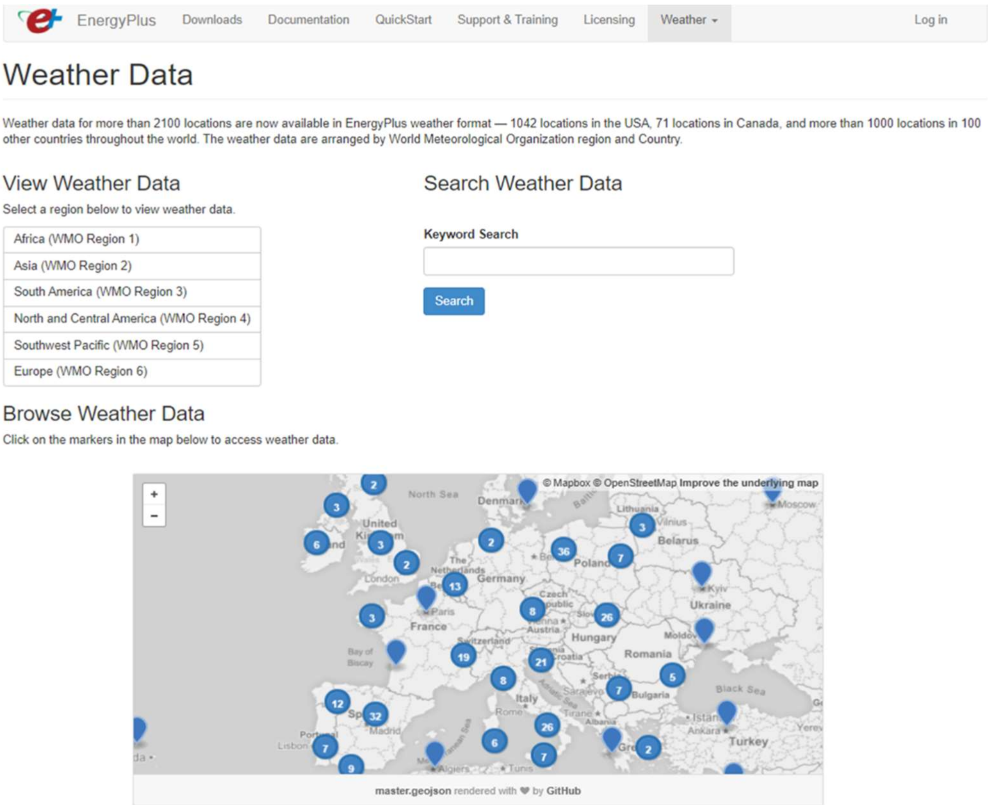

Figure 16 Opening page of the EnergyPlus weather data website, with the number of meteorological files available for different European locations

3 Characterization and Definition of Building Typologies

Different criteria are available to define residential building typologies. This section highlights those that are more useful towards the design of an energy storage system, and helps to characterize the market in which MiniStor will be offered. The housing stock in the EU is diverse and has been analysed through different perspectives, with detailed analysis mostly done for research projects related to building refurbishment. However, reliable and updated data for the whole region can be found with limited availability. The last housing-specific census at EU-level took place in 2011, with the next one being scheduled for 2021 (Eurostat, 2019). The most recent EPBD directive is recommending a renovation strategy for each country involved (EU Commission, 2019). Having as objective new updated energy reduction targets can lead to new updated national surveys that characterize better the existing building stock.

With the aim of providing the most updated scenario possible (2016,2017,2018), more databases were analysed for the buildings classification. For example, the EU Building Observatory (BSO) which directly collected data in the frame of the EU projects results such as Hotmaps[1], ODYSSEE-MURE[2]. This section includes some details for specific demo site countries, in order to illustrate the complexity of the situation.

Before analysing the classification of buildings by typologies, age, surface and heating system, it is interesting to evaluate where the largest number of the residential buildings are in the European context. Figure 17 Number of residential households in EU, UK and Switzerland [3] shows the distribution of the residential buildings in Europe[3]. Those distributions represent the key markets of households as Germany, France, Italy, Spain and UK.

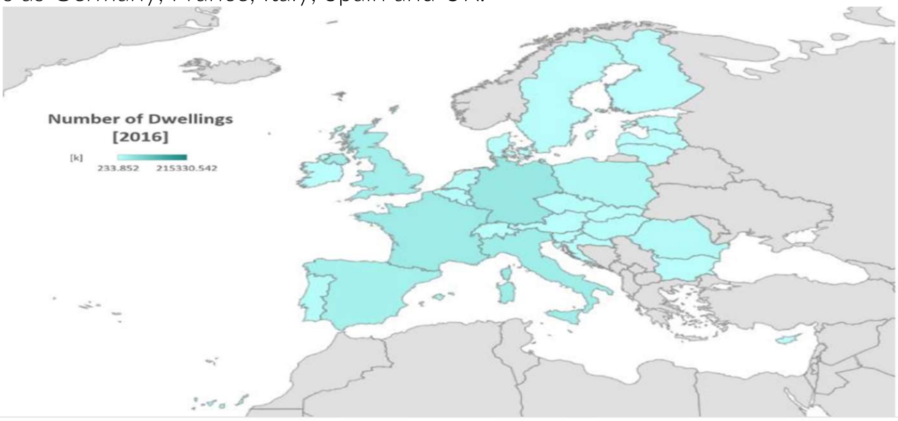

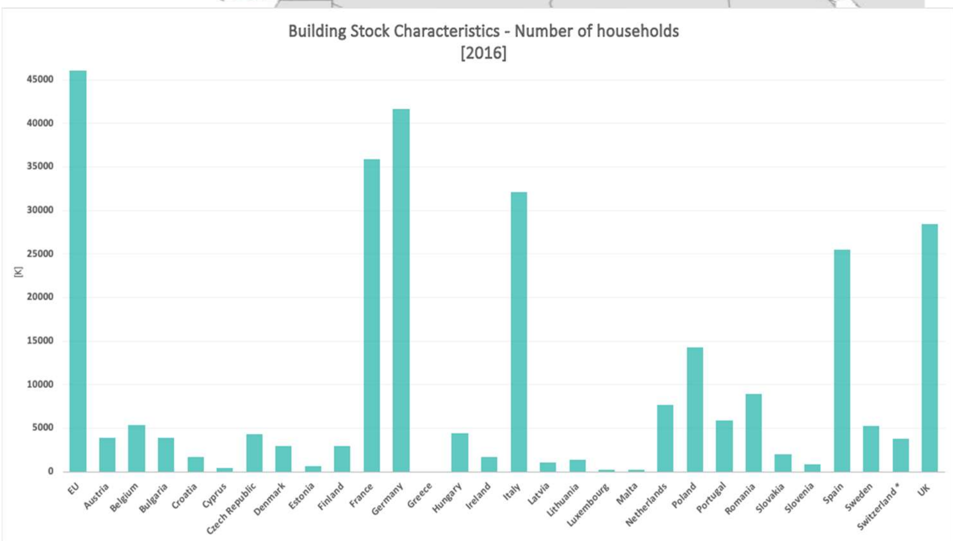

[1] Hotmaps: https://www.hotmaps-project.eu/

[2] ODYSSEE-MURE: https://www.odyssee-mure.eu/

[3] Source: ODYSSEE (online data code: https://odyssee.enerdata.net/database/)*Switzerland Source online: www.statista.com/statistics/918580/number-of-households-switzerland

Figure 17 Number of residential households in EU, UK and Switzerland [3]

3.1 Characterization of the housing stock through type of dwelling

Residential structures can be classified according to their volume type and how many units are contained within this volume. By this classification it is possible to distinguish three main types of residential buildings:

- A single detached house: It is a house not attached to any other dwelling or structure – One dwelling building.
- A semi-detached house: It has attached another dwelling side by side (or back to back) but no dwellings either above it or below it – Two dwelling building.
- A flat: It is a dwelling unit in an apartment building which has fewer or more (Hight –rise) than five storeys, or in general in a building with more than 3 dwelling.

By this classification, a global vision of the total number of buildings is reported in the Figure 12, with reference to the European census 2011. The distribution of dwellings according to type in EU countries and the UK is shown in the figure below:

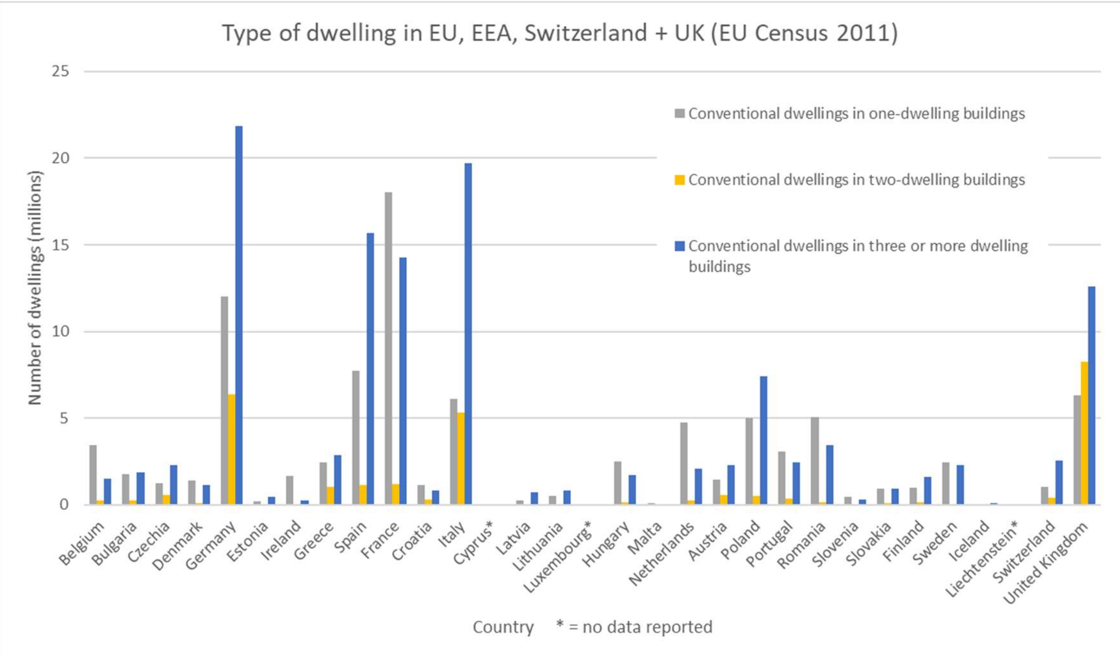

Figure 18 Classification of the housing stock in the EU and UK through type of dwelling (conventional dwellings only). Source: European Statistical System, European Census 2011

From the graph above, it can be seen that in the EU and UK the dominating building typology is that of apartment types (three or more dwellings in a building). They also make the bulk of the European building stock in key markets such as Germany, Spain, France, Italy, the United Kingdom and Poland. Those markets coincide with large numbers of detached houses as well. Typologies such as the semi-detached house are significant in the United Kingdom, Germany and Italy. A more in-deep analysis of the building classification can be obtained by the distribution of population reported by Eurostat in 2018 in the database ilc_lvho01[4] which is shown in the next figure:

[4] Eurostat ilc_lvho01 : https://appsso.eurostat.ec.europa.eu/nui/submitViewTableAction.do

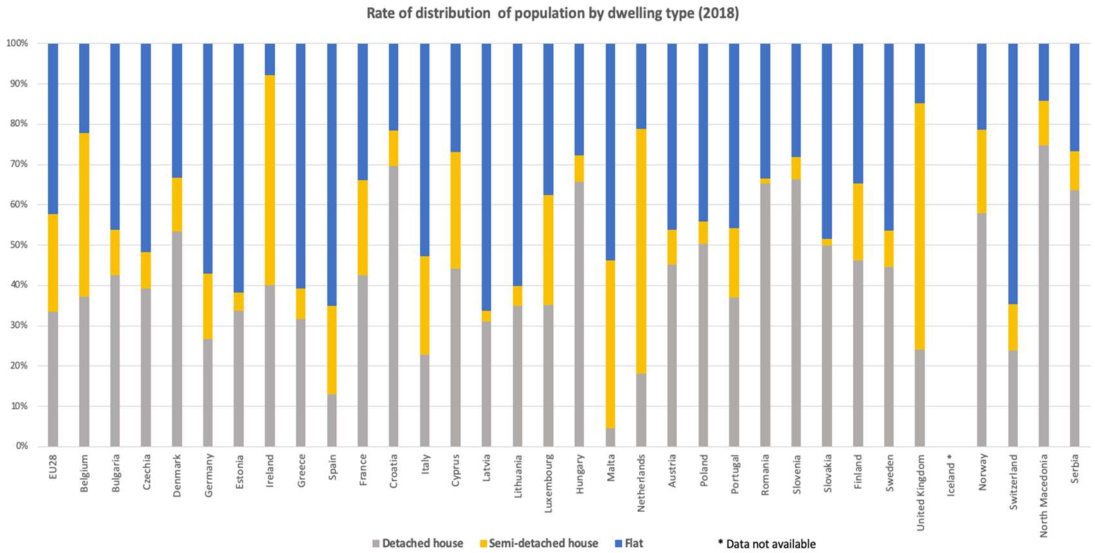

Figure 19 – Distribution of the population by dwelling types. Source: EUROSTAT ilc_lvho1

In 2018, more than 42% in the EU-28 live in flats, close to 24% in semi-detached houses and over than 33% in detached houses. The peak of people living in detached houses is in North Macedonia, (over than 70%) followed by Croatia, Slovenia, Romania, and Hungary. The proportion of people living in semi-detached house was reported in the UK (over than 60%), Netherlands, Ireland, Belgium, and Malta. While in EU countries such as Latvia, Spain, Estonia, and Greece, the majority of people live in flats.

The analysis conducted shows how the location trend of buildings could be a relevant analysis indicator with respect to Ministor project such as the energy performance and the possibility to installation of renewable plants as PV or ST panels. Flats in this context are more penalized compared to the dethatched houses for the limited space on the rooftop.

With the same aim another indicator can be the building location represented as the percentage of residential buildings by the degree of urbanization.

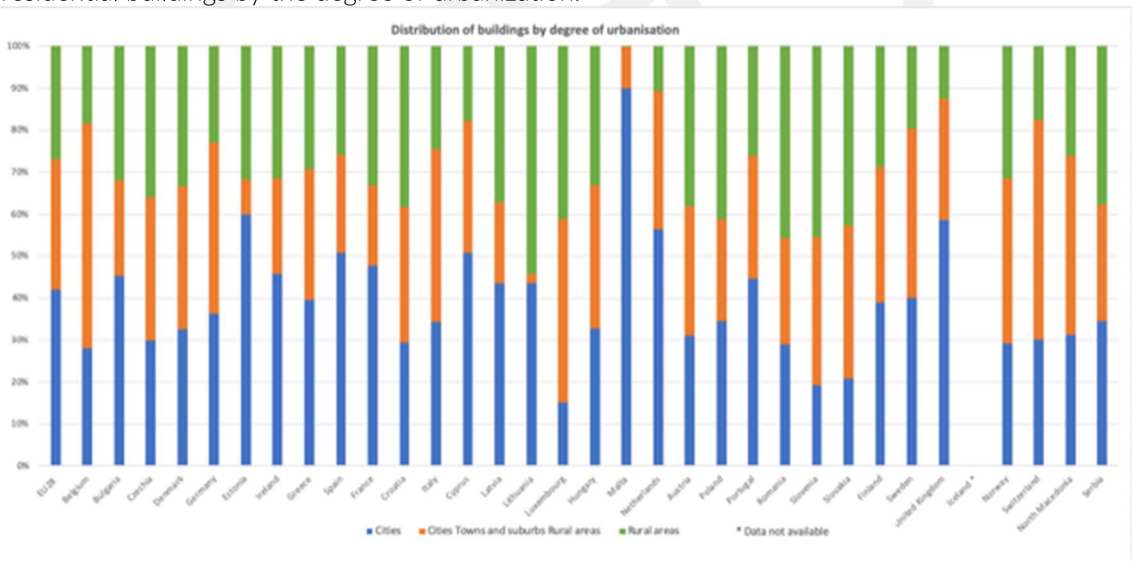

Figure 20– Distribution of buildings by the degree of urbanization. Source: EUROSTAT ilc_lvho1

In the urban context within the advent of smart grids, the economy is playing in a large scale with renovation activities able to involve buildings, streets, districts and localities, but in some cases, there are several restrictions for the renewable systems. The thinly populated areas are not able to benefit from economy measures such as in the densely-populated areas, but on the other hands have minor barriers for the implementation of renewable systems.

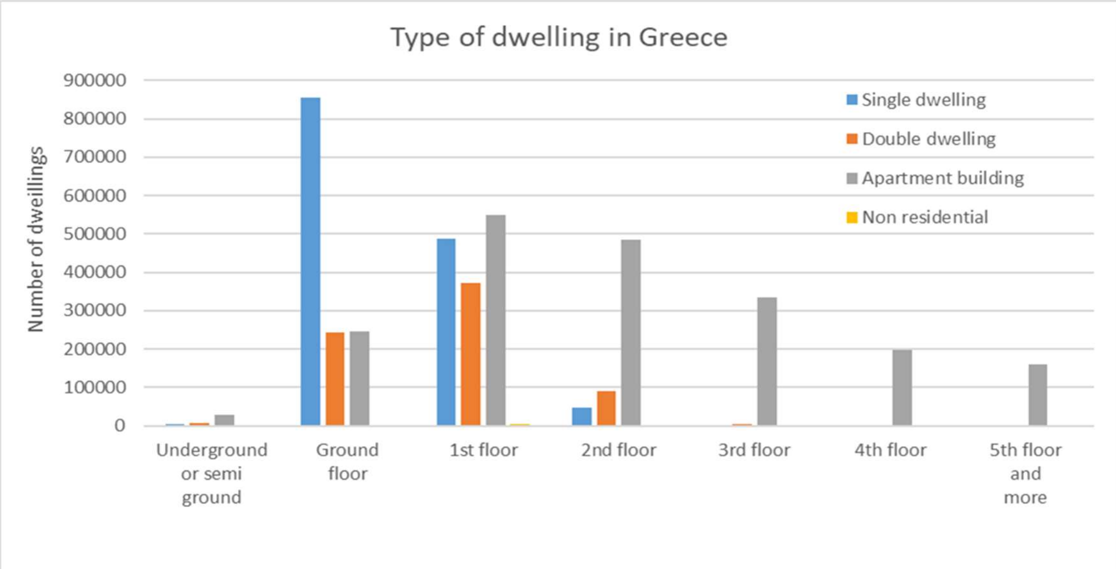

Figure 21 Number of main residences per number of floor and building type in Greece for 2011. Source: (Gaglia et al., 2018)

In the graph above, it can be observed that in Greece, the dwelling distribution per building type follows the same pattern with the European one. The main residences numbered approximately 4.1 million in 2011 and they commonly have a ground floor (32.7%) or ground floor and first floor (34.3%). Almost half of them (48.5%) are in apartment buildings (with three or more dwellings in a building), whereas a significant portion (33.8%) are in single-dwelling buildings (Hellenic Statistical Authority, Athens 2015). The case of Greece illustrates the degree of complexity of how the situation can be analysed for each demo site.

3.2 Characterization of the housing stock through age of building

This type of classification is useful to provide an insight into the existing thermal characteristics of residential dwellings, such as levels of insulation and ventilation. Usually older buildings are badly insulated, with a typical U-value (Thermal Transmittance) and infiltration rate can be proposed for each age band in every country. Such features have the potential to affect system effectiveness in terms of required energy output (more heat needs to be generated to reach a comfortable temperature in a building with insufficient insulation than in a better insulated one).

The breakdown into decades was made assuming that existing buildings before 1945 would be considered heritage buildings, therefore subject to special renovation measures. Those made between 1946 and 1990 would comply with different energy-saving measures of their time, but would still not be totally energy efficient. Buildings erected from 2006 onwards would have a higher energy efficiency as they would implement new measures such as the first versions of the EPBD.

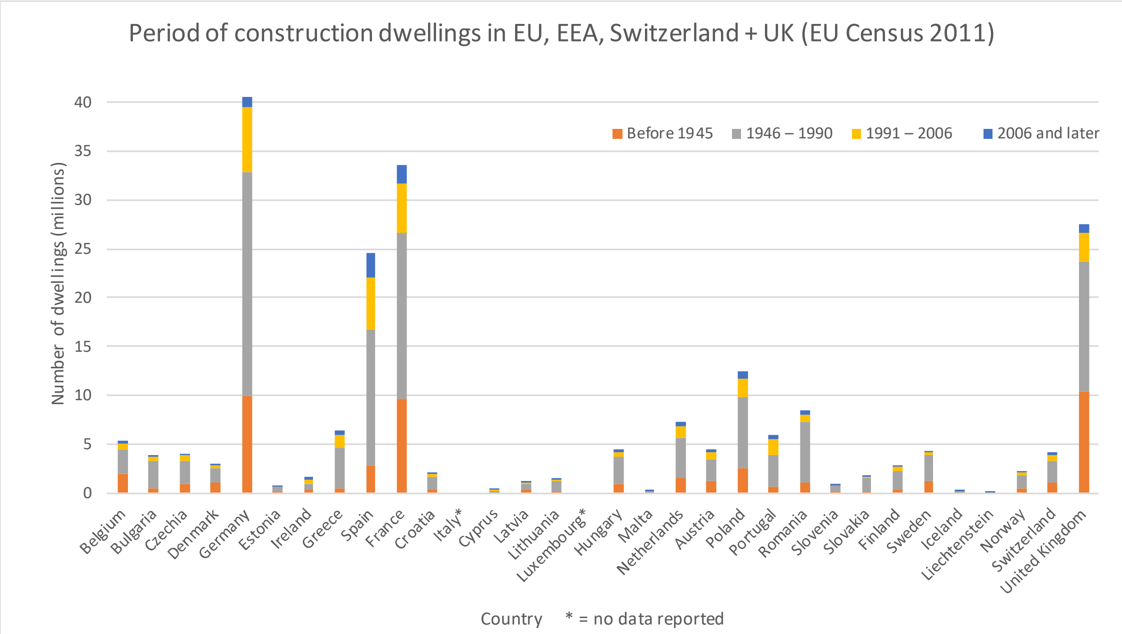

Figure 22 Classification of the housing stock in the EU and UK through age of building. Source: European Statistical System, European Census 2011

From the graph above it can be seen that in the EU and UK, the bulk of residential dwellings was built between 1946 and 1990, meaning they do not have the energy efficiency levels desired nowadays. The largest number of recent residential buildings can be found in Germany, France and Spain. But those same countries, together with the United Kingdom, Poland and Romania, possess the largest number of residential buildings made between 1946 and 1990.

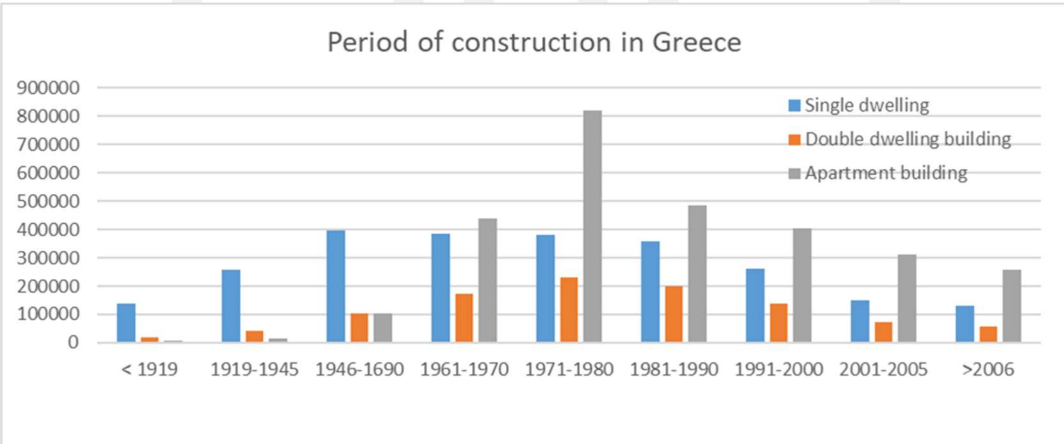

Figure 23 Classification of the housing stock in Greece per type through age of building. Source: (Hellenic Statistical Authority, Athens 2015)

In the figure above, the classification of housing stock in Greece per dwelling type and construction year is presented for the year 2011. This figure regards all the dwellings (approximately 6.3 million) and not only the main residences. A small portion of them (7.6%), mainly single-dwelling buildings, were built before 1946. Similar to the EU and UK trends, the vast majority of dwellings (64.3%) were constructed in the period 1946-1990. After 1961 the majority of new dwellings concerns apartment buildings. In general, dwellings in Greece are characterized by low energy efficiency as only 7% of them were built from 2006 onwards. Noteworthy is the fact that after 1980, a steady decrease of the construction of new buildings is observed.

This project has received funding from the European Union's Horizon 2020 research and innovation programme under grant agreement No 869821

The implications for future development of the MiniStor system involve that its effectiveness in most existing buildings will be greatly improved if it is offered as part of a building renovation package, whereas its effect might have certain limitations if those buildings are not well-insulated or with high infiltration rates. This needs to be corroborated at the demonstration and market feasibility study stages.

3.3 Characterization of the housing stock through existing useful area

Another way of classifying the residential building stock is through the useful area of dwellings. This will impact the volume that needs to be conditioned as living space, determining power output requirements, location within the dwelling, etc. The categories recorded in the census were summarized in this report to the most common areas, such as between less than 30 to less than 50 m², 50 to less than 100 m², 100 to less than 150 m², and dwellings of 150 m² or more. The distribution is shown in the graph below:

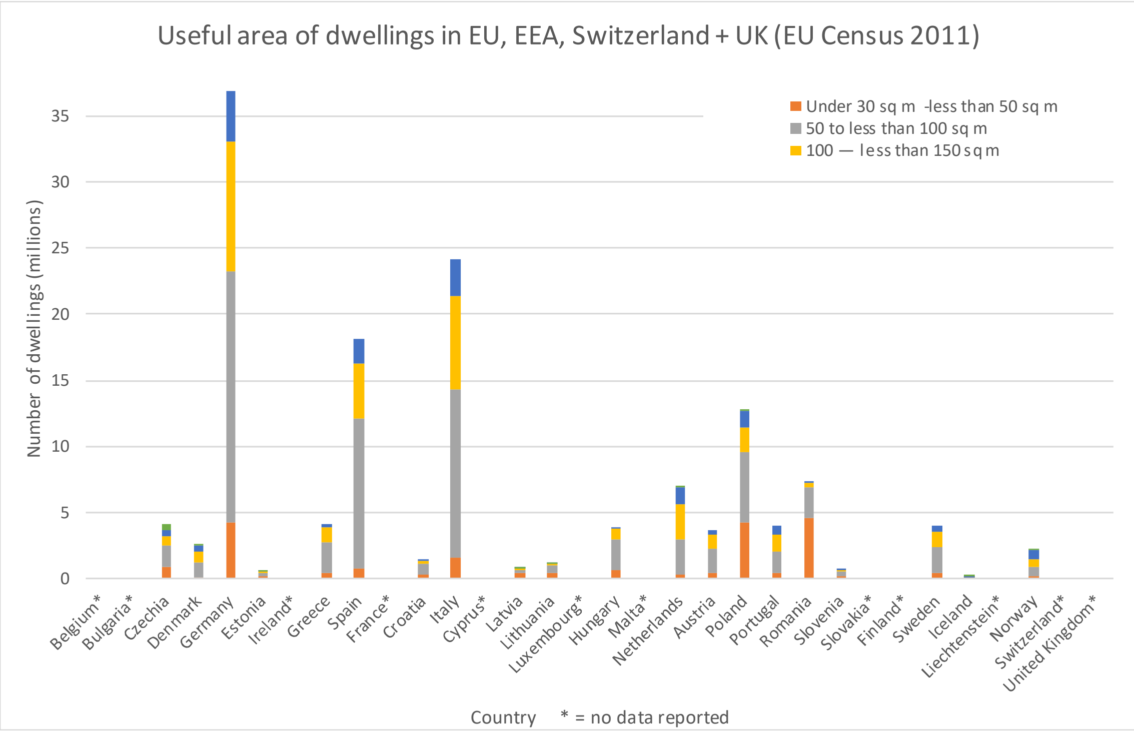

Figure 24 Classification of the housing stock in the EU and UK through useful area. Source: European Statistical System, European Census 2011

According to this figure, the most common size of dwellings in the EU consist of those with a useful area between 50 to 100 m², while the second most common are those between 100 to 150 m². Most of both categories are found in Germany, Spain and Italy. It must be noted that in certain Eastern European countries such as Poland and Romania, apartments with useful area of less than 30 to 50 m² constitute a significant amount of their building stock. Data for this feature was not recorded in various countries such as the UK, Ireland and Belgium, therefore the category is empty.

The next figure shows an interesting statistic regarding the average size of dwellings in cities, towns, and suburbs or rural places. The biggest difference is recorded in Luxembourg followed by Belgium which confirms with Sweden the higher size of dwellings both in rural and city contexts.

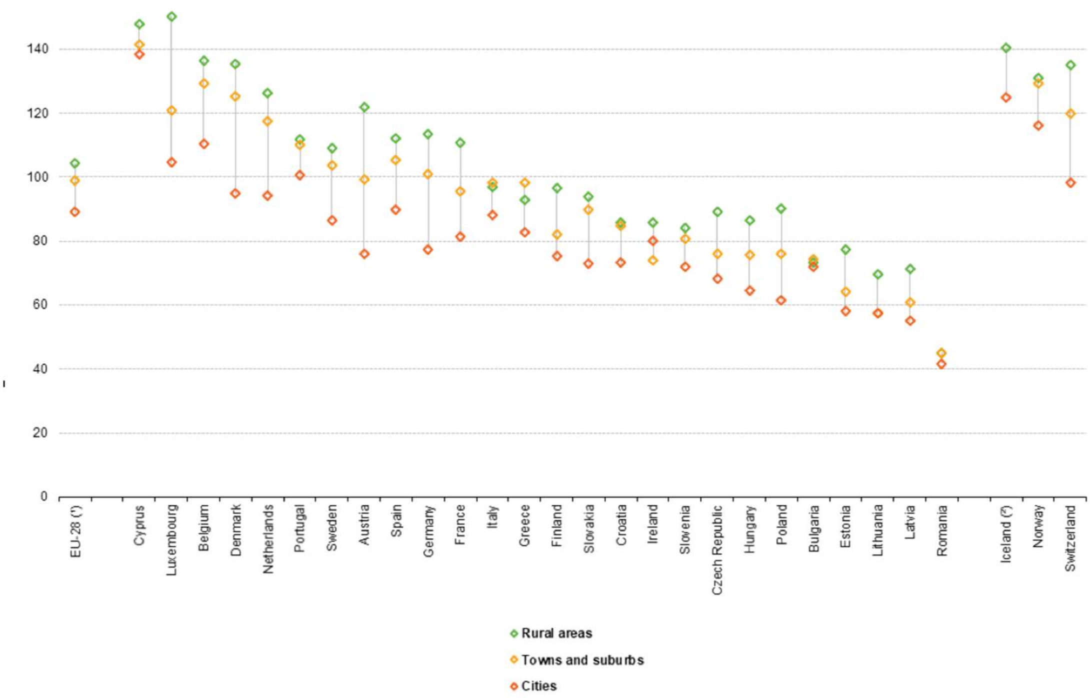

Figure 25 – Average size of dwellings by degree of urbanization 2012 in m²- Source: Eurostat (online data code: ilc_hcmh02)

Figure 26 presents the number of main residences and their total floor area (m²) per dwelling type as was reported in Greece in 2011. According to the graph, the most common size of dwellings is between 51 and 120 m². Many of the dwellings in apartment buildings (31.3%) have a useful area between 71-90 m². On the other hand, a significant portion of main residences in single- and double-dwelling constructions, 26.4% and 32.3% respectively, present useful areas in the range of 91 to 120 m². A small portion (13.7%) of the main residences have useful area lower than 50m².

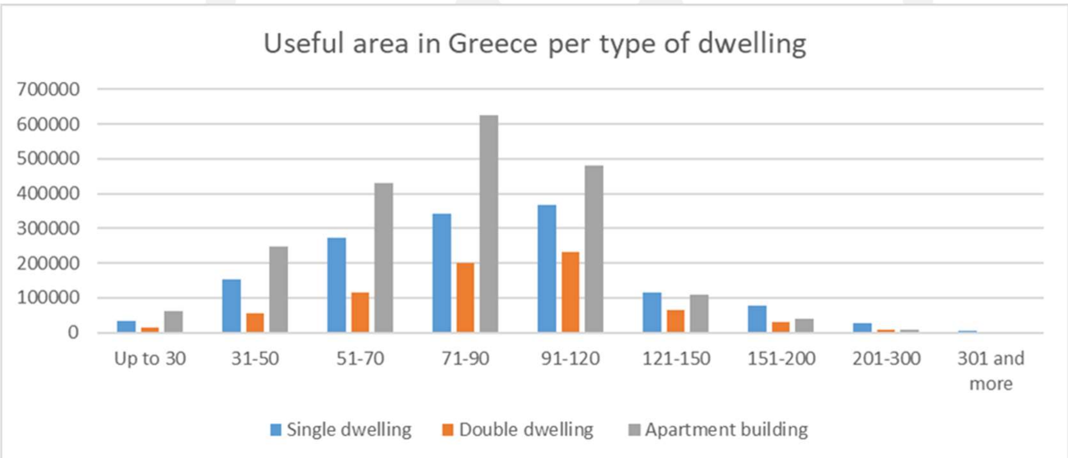

Figure 26 Classification of housing stock per type in Greece through useful area. Source: (Gaglia et al., 2018)

3.4 Characterization of the housing stock through existing heating system

Since MiniStor will integrate with existing heating systems, it is useful to know about which are the main types to be found in the European area. The census categories, however, have as categories the presence or absence of a central heating system. This does not necessarily mean that all dwellings do not have a heating system at all. Central heating systems can include technologies such as boilers, district heating, heat pumps, etc. Distributed heating systems can be considered such as those offered by window HVAC units, where the space adjacent to it is conditioned. The results of the census are shown in the following figure:

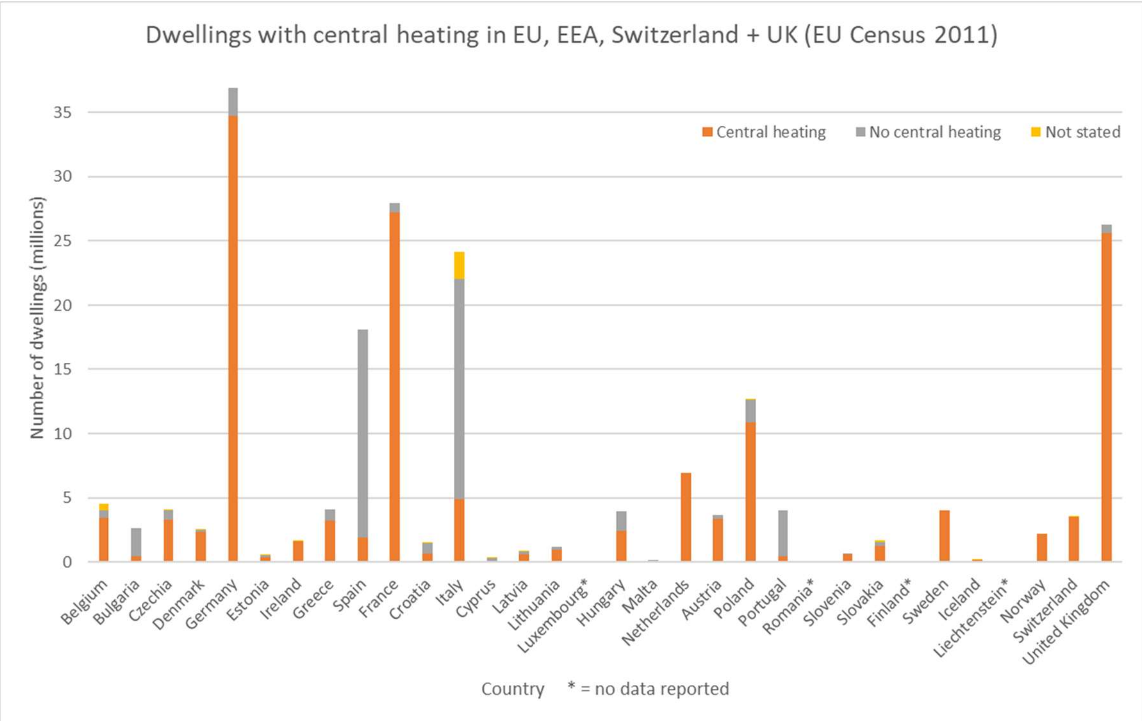

Figure 27 Classification of the housing stock in the EU and UK through existing heating system. Source: European Statistical System, European Census 2011

The graph shows that central heating systems are overwhelmingly dominant in almost all European countries, with the highest numbers found in Germany and France, where almost all the housing stock has a central heating system. However, markets such as Spain, Italy and Portugal have as the dominating category the "no central heating". It can be inferred that due to their climate, dwellings in those countries require systems that can also provide both heating and cooling during the year. This is usually solved through commercially-available HVAC units that are fitted to one or several rooms. The presence of existing central heating systems allows for easier integration of MiniStor into these systems.

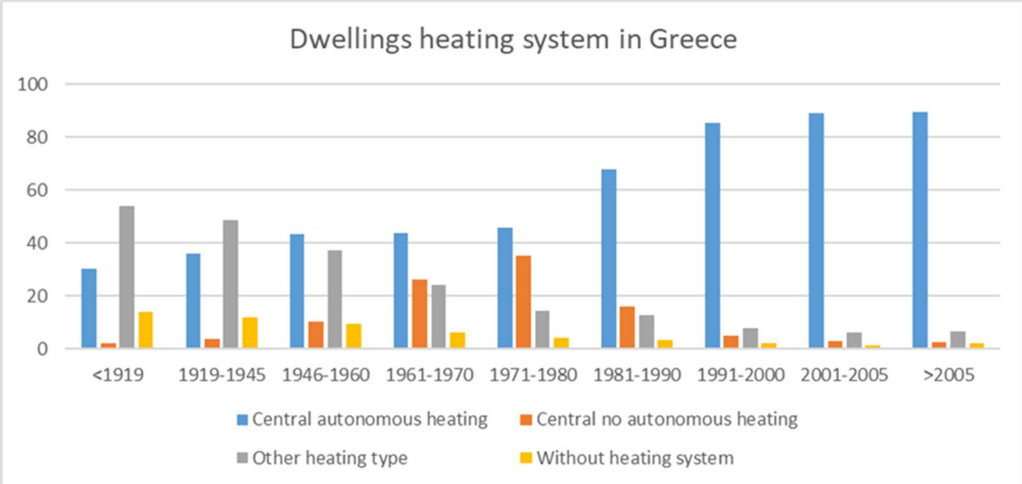

Figure 28 Classification of the housing stock in Greece through existing heating system and year of construction. Source: (Gaglia et al., 2018)

The above figure presents the percentage of the housing stock in Greece per type of existing heating system and year of construction, as was reported in 2011. Similar to Figure 23 the mentioned data regard all the dwellings. The construction period affects considerably the used heating system. The majority of buildings built before 1945 and 20.3% of the total dwellings, use heating systems other than central heating (electric heaters, grates, heat pumps etch.). Approximately 67.7% of all dwellings have central space heating system (individual or collective), but this percentage rises to about 70% for the dwellings built after 1960 and reaches 90% for residential buildings constructed after 1990. Only 12% of the housing stock do not have or use any heating system (Gaglia et al., 2018).

Previous figures provide an overview of the physical conditions where the system will operate, and can provide initial insights for future commercialization efforts. As such, on an initial stage it can be seen the large potential to supply a sustainable energy storage solution.

4 Characterization of User Profiles

An important factor for consideration in the sizing of the system are the heating and cooling loads that must be provided in order to keep occupants comfortable in residential buildings, as well as the heating loads brought from occupants carrying out activities within them. Other factors that are not related to building characteristics but impact system design, comprise number of occupants that might be present, their ventilation needs, equipment being used in a space, and lighting demands.

This section, which aims to be a summary for commonly accepted values and not an exhaustive compendium, has as relevant sources handbooks and publications of professional bodies such as ASHRAE. These values represent the basis to form user profiles as needed in future calculations that will be performed in other Work Packages.

4.1 Occupancy in Residential Buildings

4.1.1 Occupancy Density

Estimates on number of occupants have been made by ASHRAE in Standard 62.1-2019 "Ventilation for acceptable Indoor air quality"(ANSI/ASHRAE, 2019a) and Standard 62.2-2019 "Ventilation and Acceptable Indoor Air Quality in Low-Rise Residential Buildings"(ANSI/ASHRAE, 2019b). Standard 62.1 provides estimates based on area as shown in Table 15, while Standard 62.2 provides estimates based on number of bedrooms in a dwelling, independent of its size.

Occupancy category Hotels, Motels, Resorts, Dormitories	Occupant density Per 100 m^2
Barracks sleeping areas	20
Bedroom/living room	10
Laundry rooms, central	10
Laundry rooms within dwelling units	10
Lobbies/prefunction	30
Multipurpose assembly	120

Table 15:Occupancy density for different residential-type categories. Source: ASHRAE Standard 62.1

Standard 62.2 specifies that the first bedroom which has access to full services such as kitchen and bathroom must have a maximum occupancy of 2 persons. Every additional bedroom is estimated to have an occupancy of 1 person. However, it is acknowledged in the same standard that this figure has to adapt to the maximum allowed by local councils in each area.

4.1.2 Occupancy schedules

The dynamics of occupants within the building can be abstracted by stating when and how many occupants are to be found within a building or space. This is useful to know the times when stored heat must be released and when it can be stored more efficiently. Predicting occupancy, however, is not accurate since different people have different occupancy patterns that also vary with the year. For ASHRAE, the most usual patterns are used, which assume a large number of family members being outside of home mostly during daytime hours and gradually returning for night-time. To account for people staying at home, low occupancy is assumed between 10:00 to 15:00hrs. This pattern is used for all days of the year.

Meanwhile, the SIA-Arbeitsblatt 2024 from the Swiss Society of Engineers and Architects (SIA, 2015) proposes an occupancy pattern where residents stay at home during night time hours, but return for lunchtime (12:00-14:00hrs). The dwelling is occupied in steps again during the afternoon (from 17:00hrs onwards). The pattern is repeated for all days of the year as well. Depending on the usage type the occupancy patterns are adjusted to account for higher occupancy of residential space during the weekend.

Since these types of values are useful in energy simulations, different interpretations have been taken by software providers. For example, the Revit software provides some typical occupancy schedules for residential buildings, and are based on ASHRAE. They are stated per 100 persons in a given building type (Autodesk, 2019). For its part, TRNSYS uses the interpretation given by SIA in its schedules for home occupancy (Thermal Energy System Specialists, 2019)

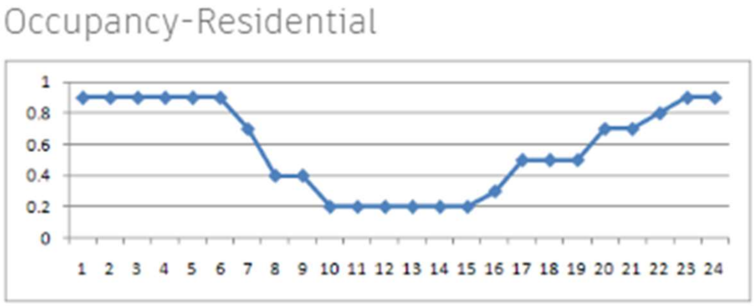

Figure 29 Daily residential occupancy profile in Revit software according to ASHRAE

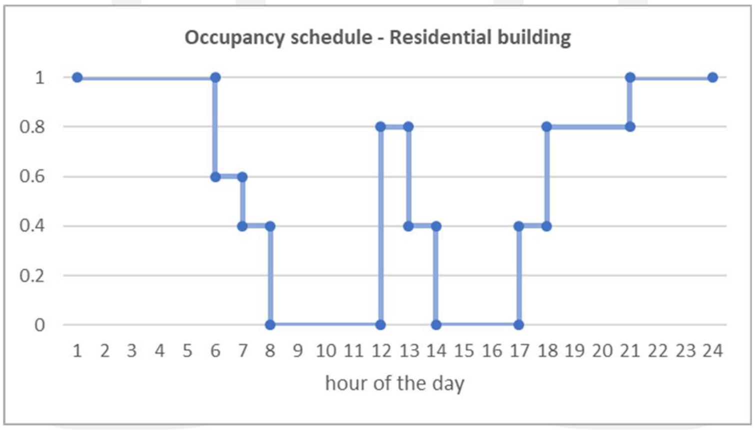

Figure 30 Daily residential occupancy profile in TRNSYS software according to SIA 2024

Modelling the occupancy in a building depends strongly on the actual usage of the building as well as the behaviour of the occupants. Therefore, only very little normative work or prescriptions could be identified. One available standard suggesting occupation profiles is the SIA-Arbeitsblatt 2024 from the Swiss Society of Engineers and Architects (SIA, 2015). This document defines standard profiles of usage, occupation as well as standard appliance loads for different usage cases. Since MiniStor focuses on residential buildings, only single-family homes and apartment buildings are described. According to SIA 2024 the typical percentage of surface use in an apartment building is 90% in living space and bedrooms and 10% in traffic area.

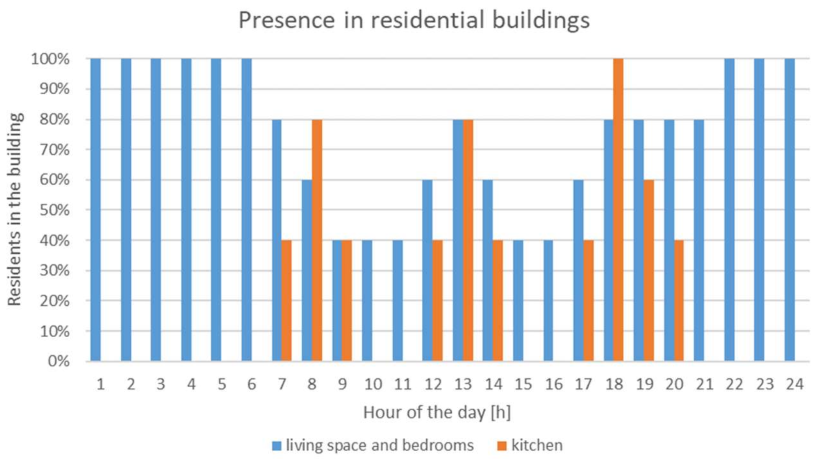

Figure 31 Daily residential occupancy profile according to SIA 2024

4.1.3 Occupancy Gains

Heat gains due to occupancy represent a portion of the total internal heat gains of a building that have to be taken into account when calculating the corresponding cooling needs. In some building typologies related to high occupancy levels, occupancy gains can affect considerably the required cooling loads. These gains are related to the heat that the human body rejects to the environment in the form of sensible heat and moisture in an effort to keep its temperature constant. The rate at which the heat is emitted to the environment is related to various factors that can be classified into personal (type of activity, clothing) and environmental ones (air temperature and velocity, humidity, mean radiant temperature of human body) (Arendt, 2012). The Table 5.2.1.2 of ASHRAE Standard 55 (ANSI/ASHRAE, 2017), "Thermal environmental conditions for human occupancy" gives the metabolic rates of the occupants for different types of tasks. The following table shows some selected activities that would be pertinent for the residential setting.

Activity	Metabolic rate (W/m^2)
Resting	
- Sleeping	40
- Reclining	45
- Seated, quiet	60
- Standing, relaxed	70
Office activities	
- Reading, seated	55
- Writing	60
- Typing	65
- Filing, seated	70
- Filing, standing	80
- Walking about	100
- Lifting/packing	120
Miscellaneous Occupational Activities	
- Cooking	95-115
- House cleaning	115-200
- Dancing, social	145-255

Table 16 Metabolic rates for different activities in a residential context. Source: ASHRAE Standard 55

Furthermore, Table 1 / Chapter 18 of ASHRAE Handbook Fundamentals (2017) gives some representative rates at which heat and moisture are rejected by the human body to the environment during different activities. Some of them, related to activities that take place in residential dwellings, are summarized in the following table. The depicted values are based on a 24°C room dry-bulb temperature, they are round to nearest 5 W and refer to the adjusted heat gain based on normal percentage of men, women, and children for the application listed, assuming that gain from an adult female is 85% of that for an adult male, and gain from a child is 75% of that for an adult male.

Degree of Activity	Location	Total Heat (W)	Sensible Heat (W)	Latent Heat (W)
Seated, very light work	Office, hotels, apartments	105	70	45
Moderate active office work	Office, hotels, apartments	130	75	55
Standing, light work, walking	Department store, retail store	130	75	55
Walking, standing	Drug store, bank	145	75	70
Moderate dancing	Dance hall	250	90	160

Table 17. Representative rates of heat rejection by human body in states of activity pertinent to residential dwellings. Source: ASHRAE Handbook Fundamentals

On the other hand, the SIA directive 2024 proposes the following assumptions for an apartment and for an individual dwelling:

Condition	Apartment	Detached house	Unit
Occupants			
- Occupied hours per day	17	17	h
- Fully occupied hours per day	14	14	h
- Days in use per year	365	365	d
- Fully occupied hours per year	4090	4090	h
- Surface per person	30	30	m^2
- Metabolic activity	1.2	1.2	met
- Internal gain per person	2.3	1.4	W/m^2

Table 18 Metabolic activity and internal gain per person. Source: SIA-2024

4.2 Ventilation Rates

Ventilation is the process of replacing the indoor air of a space with fresh outdoor air. It can be provided by natural effects (wind, thermal or diffusion effects) and / or by special mechanical equipment. Although it is a necessary procedure in order to keep indoor air quality in acceptable levels, it has a negative effect on the thermal and cooling space requirements as it involves the replacement of indoor air with air of ambient temperature.

4.2.1 All buildings except low-rise residential buildings

ASHRAE 62.1 (2019) standard "Ventilation for acceptable Indoor air quality" is related to the ventilation in all building types except from low-rise residential ones. According to this standard the minimum required ventilation rate V_s of a space is defined by the following equation:

$$V_s = R_p \times P_z + R_a \times A_z$$

, where P_z and A_z are the number of people within the space and the space area respectively. This equation applies to new buildings and additions to existing buildings, and to all types of buildings with the exception of residential occupancies in which the occupants are nontransient (i.e. they own the building, lease it or rent it for periods of one month or more). In cases where the variable P_z is not known, typical values of the occupancy density are given in Table 6.1 of the aforementioned standard. The coefficients R_p and R_a represent the required outdoor airflow rate per person and area respectively. Their values vary according to the space use and are depicted also in Table 6.1 of ASHRAE 62.1. Data extracted from this table, pertinent to residential usage, are summarized in Table 19.

Occupancy category	People outdoor air rate R_p	Area Outdoor Air rate R_a	Occupant density
Hotels, Motels, Resorts, Dormitories	l/s x person	L/s x m^2	#/100 m^2
Barracks sleeping areas	2.5	0.3	20
Bedroom/living room	2.5	0.3	10
Laundry rooms, central	2.5	0.6	10
Laundry rooms within dwelling units	2.5	0.6	10
Lobbies/prefunction	3.8	0.3	30
Multipurpose assembly	2.5	0.3	120

Table 19. Occupancy density and minimum outdoor air rates for different residential-type categories. Source: ASHRAE 62.1

In several space typologies the required air ventilation is defined by estimating the minimum air exhaust, i.e. the minimum required removal of indoor air from the space and its discharge to the outdoor. In these cases the required air renewal is mainly depended on the space area. The corresponding coefficients are presented in the Table 6.2 of ASHRAE 62.1 (2019) and information relevant to hotels, motels, resorts and dormitories are displayed in the table below.

Occupancy category	Exhaust rate	
Hotels, Motels, Resorts, Dormitories	l/s x unit	L/s x m^2
Janitor closets, trash rooms, recycling		5
Kitchenettes		1.5
Shower rooms	10/25	
Parking garages		3.7
Residential kitchens	25/50	
Soiled laundry storage rooms		5
Toilets – private	12.5/25	
Toilets - public	25/35	

Table 20. Minimum exhaust rates for different residential-type categories. Source: ASHRAE 62.1

4.2.2 Low rise residential buildings

A low rise residential building is defined by ASHRAE as any residential building that has less than four stories.

In this type of buildings, the total required airflow rate that a ventilation system has to provide is calculated as a function of the dwelling area and the number of bedrooms. According to ASHRAE 62.2 (2019) standard "Ventilation and acceptable indoor air quality in low-rise residential buildings", the following expression can be used:

$$V_s = 0.15 \times A_{floor} + 3.5 \times (N_{br} + 1)$$

where A_{floor} and N_{br} are the dwelling-unit floor area and the number of bedrooms respectively. Alternatively, default values provided by Table 4.1b of ASHRAE 62.2 (2019) can be used.

Floor Area (m^2)	Number of bedrooms				
	1	2	3	4	5
< 47	14	18	21	25	28
47 to 93	21	24	28	31	35
94 to 139	28	31	35	38	42
140 to 186	35	38	42	45	49
187 to 232	42	45	49	52	56
233 to 279	49	52	56	59	63
280 to 325	56	59	63	66	70
326 to 372	63	66	70	73	77
373 to 418	70	73	77	80	84
419 to 465	77	80	84	87	91

Table 21. Ventilation air requirements (L/s). Source: ASHRAE 62.2

The values calculated with the above equation and depicted in Table 21, are valid under the assumption of two persons in a studio or one-bedroom dwelling unit and one additional person for each additional bedroom. In cases of higher occupant densities, the resulting ventilation rate should be increased by 3.5 L/s for each additional person. In general, the minimum required airflow rates in the cases of residential buildings are significantly higher than those of the other non-residential building typologies.

Regarding minimum exhaust airflows, ASHRAE standards consider the installation of local mechanical exhaust systems in each kitchen and bathroom of a residential dwelling. This system could be either demand-controlled or operate continuously. The minimum airflow rates in the first case are displayed in Table 5.1 and in the latter case in Table 5.2 of ASHRAE 62.2 (2019) standard. The relevant data are summarized in the tables below. As it can be observed, the required airflow of continuously operating systems is considerably lower than that of the controlled ones.

Application	Airflow
Enclosed kitchen	- Vented range hood (including appliance-range hood combinations): 50 L/s - Other kitchen exhaust fans, including downdraft: 150 L/S or a capacity of 5 air changes per hour
Non-enclosed kitchen	- Vented range hood (including appliance-range hood combinations): 50 L/s - Other kitchen exhaust fans, including downdraft: 150 L/S
Bathroom	25 L/s

Table 22. Demand controlled local ventilation exhaust airflow rates. Source: ASHRAE 62.2

Application	Airflow
Enclosed kitchen	5 air changes per hour, based on kitchen volume
Bathroom	10 L/s

Table 23. Continuous local ventilation exhaust airflow rates. Source: ASHRAE 62.2

The SIA directive 2024 provides the following assumptions for an apartment building and for an individual dwelling:

Ventilation	Apartment Dwelling	Individual Dwelling	Units
- Fresh air flow per person	30	30	m^3/ h
- Fresh air flow per net floor surface	1	0.6	$m^3/(m^2\ h)$

-	Infiltration air flow	0.15	0.15	$m^3/(m^2\ h)$
-	Control of ventilator	1	1	Speed
-	Electrical Power of the fan	0.3	0.2	W/m^2
-	Full load hours per year	4120	4120	h
-	Annual ventilation demand	1.2	0.7	KWh/m^2

Table 24 Ventilation requirements in apartment and individual dwellings. Source: SIA 2024

4.3 Lighting loads

4.3.1 Lighting Power Densities and gains

Lighting represents a significant portion of the energy consumption in buildings. In addition, lighting produces heat gains that must be taken into account when calculating the cooling needs of a space. Therefore, ASHRAE has set up maximum allowable lighting power densities (LPD) with which the interior and exterior lighting design of new and renovated constructions has to comply. According to ASHRAE latest version of standard 90.1 - Energy standard for buildings except low-rise residential buildings (ANSI/ASHRAE, 2019c), which applies to all building typologies except from low-rise residential dwellings, there are two methods to calculate the interior lighting power allowance: a) the Building Area Method Compliance Path and b) the Space-by-Space method. The latter one is more accurate, however the first method combines simplicity with reasonable accuracy. According to the Building Area Method Compliance Path, the appropriate building area type is firstly determined and the corresponding allowed LPD is selected from values of Table 9.5.1 of the standard. As a next step, the gross lighted area of the building area type is determined and then is multiplied with the allowed LPD. The interior lighting power allowance of the whole building is the sum of the allowed LPDs of all building area types. Possible exchanges between building area types are permissible, provided that the total building LPD threshold is respected. The maximum LPDs of some relevant spaces have been extracted from Table 9.5.1 of ASHRAE 90.1 (2019) and are presented in the table below.

Building Area type	LPD (W/ft^2)
Dining: family	0.71
Dormitory	0.53
Multifamily	0.45
Parking garage	0.18

Table 25. Lighting Power Density allowances using the Building Area Method. Source: ASHRAE 90.1

In the case of dwelling units, the 90.1 standard defines that at least 75% of the permanently installed lighting fixtures of the building should use lamps with no less than 55 lm/W efficacy. Alternatively, the total luminaire efficacy should be higher than 45 lm/W. However, all the other provisions of this standard are not applicable to this type of building type.

CEN standard 15193-1 (2017) (CEN, 2017) provides minimum requirements for installed lighting power for residential buildings:

Space	Lighting type	Installed power for typical lighting solution (W)		
		Small area	Medium area	Large area
Kitchen	General and ambient lighting	60	80	120
	Worktop lighting	90	90	90

Dining room	General and ambient lighting	100	135	200
	Dining table lighting	120	120	120
Living room	General and ambient lighting	100	135	200
	Reading light	60	60	60
Bathroom and toilets	General and ambient lighting	50	70	100
	Mirror lighting	70	70	70
Bedroom	General and ambient lighting	90	110	140
	Bedside lamps	30	30	30
	Desk lamps	50	50	50
Entrance hall, corridors and stairs	General and ambient lighting	40	60	80
Storeroom, cellar and laundry room	General and ambient lighting	60	80	120
**Indicated power value for fixed installed luminaires only*				

Table 26 Installed power for rooms in residential buildings. Source: CEN 15193-1 (2017)

4.3.2 Lighting gains

Luminaires transform electrical energy into both light and heat, which is then transferred to the environment. Different types of lamps and their setup within the ceiling provide different amounts of heat being conducted. An example is given in the table below, which comes from the Environmental Design CIBSE Guide A (Butcher et al., 2015).

Lamp type	Heat Output %	
	Radiant	Conducted/Convective*
Fluorescent	30	70
Filament (tungsten)	85	15
High pressure mercury/sodium, metal halide	50	50
Low pressure sodium	43	57
*Power loss of ballasts should be added to conducted/convective heat		

Table 27 Heat output according to lamp type. Source: CIBSE Design Guide A

4.3.3 Lighting Schedules

The distribution of lighting usage times varies according to the assumptions on when activities are being carried out. Due to the variability of daylight in dwellings, this is not uniform, but night time hours are usually taken into account for most lighting usage. This is reflected in the following table of lighting assumptions for an apartment and for individual dwelling from SAI directive 2024 (SIA, 2015)

Lighting		
- Hours of use per day (7-18 h)	4	h
- Hours of use per night (18-7 h)	3	h
- Electrical Power of lighting	2.7	W/m^2
- Internal gain of lighting	2.7	W/m^2
- Hours of full load per year	1450	h

-	Annual electric demand	4	kWh/m²

Table 28 Usage hours and lighting power assumptions according to SIA 2024

4.4 Equipment Gains

Another source for heat generation comes from the equipment present in households and which are needed to carry out activities. These range from domestic appliances such as kitchen ranges and dishwashers to small-scale office equipment such as computers and printers. Their use is also spread during the day, with certain items such as water heaters, kitchen hobs and others being used during "peak times" (usually early morning, noon and evening). Other equipment has constant use, for example refrigerators and other equipment that needs to be on standby, e.g. television sets. Therefore, the usage footprint of a household is never zero during a typical day. The following assumptions for usage and installed power come from SIA directive 2024 (SIA, 2015)

Electric equipment		Value	Units
-	Hours of full load per day	6.1	h
-	Electrical load	8	W/m²
-	Stand by load	10	%
-	Thermal load	8	W/m²
-	Full load hours per year	1780	h
-	Annual demand	14	KWh/m²

Table 29 Usage hours and installed power in a residential dwelling. Source: SIA 2024

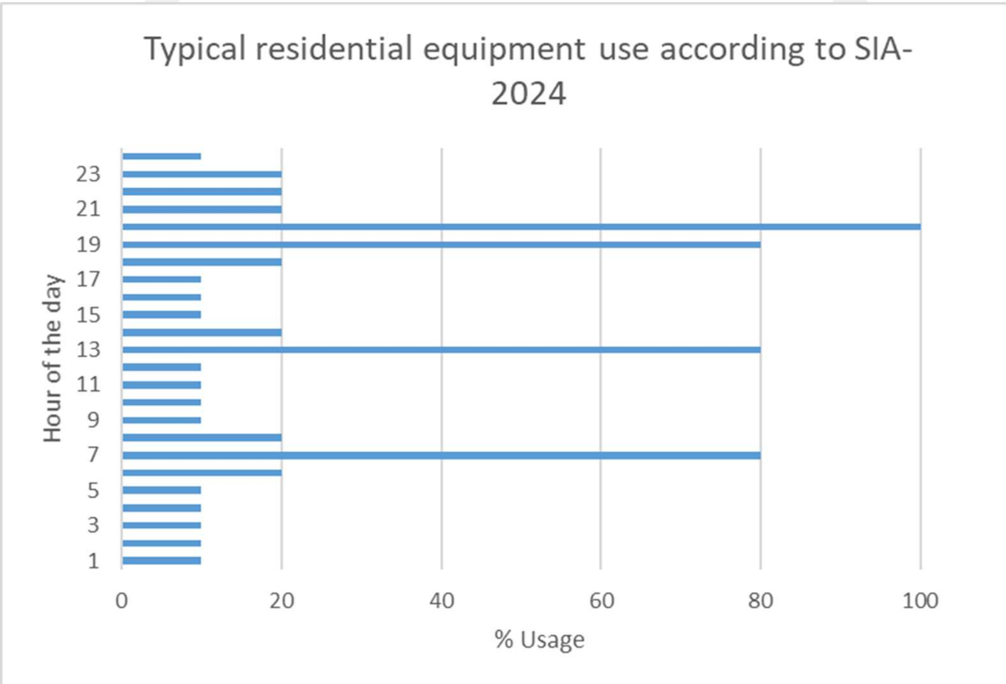

Figure 32 Typical residential equipment use during the day. Source: SIA 2024

4.4.1 Gains from specific household equipment

Equipment gains from specific household equipment can be obtained from different tables present in diverse standards. The following tables provide the most representative appliances that can be found and is not intended to be exhaustive.

Typical heat gains from office equipment is presented in the table below. They are obtained from the CIBSE Environmental Design Guide A.

Nature of value	Value for stated mode / W	
	Continuous	Energy Saving
Average PC	55	20
Small PC monitor (13-15 inch)	55	0
Medium PC monitor (16-18 inch)	70	0
Large PC monitor (19-20 inch)	80	0
Small desktop laser printer	130	10
Scanner	25	15

Table 30 Average values for office equipment commonly present in households. Source: CIBSE

To estimate heat gains from cooking appliances, the energy input rating is extracted from the manufacturer's data and multiplied by usage factors and efficiencies. The following table shows some sample cooking appliances that could be found in a residential dwelling. They are obtained from the CIBSE Environmental Design Guide A.

Appliance	Size	Energy rate / W		Rate of heat gain / W			
		Rated	Standby	Without hood			With hood
				Sensible	Latent	Total	Sensible
a) Electric, no hood required							
Blender, per litre of capacity	1.0 – 3.8 litre	480	-	310	160	470	150
Coffee brewer	12 cups / 2 burners	1660	-	1100	560	1660	530
Dishwasher (conveyor type, water sanitising)	5000-9000 dish/h	340	-	44	108	152	50
Food processor	2.3 litre	520	-	520	0	520	0
Freezer (small)	0.51 m^3	810	-	320	0	320	0
Microwave oven (residential type)	30 litre	600-1400	-	600-1400	0	600-1400	0
Mixer (small), per litre of capacity	11-72 litre	15	-	15	0	15	0
Refrigerator (small) per m^3 of interior space	0.17-0.71 m^3	1730	-	690	0	690	0
Toaster (small pop-up)	4 slice	2470	-	1310	1160	2470	790
Waffle Iron	0.05 m^2	1640	-	700	940	1640	520
b) Electric, exhaust hood required							
Broiler (single deck infrared), per m^2 of broiling area	0.24-0.91 m^2	34200	-	-	-	-	6780
Oven (roasting) per m^3 of oven space	0.22-0.66 m^3	28300	-	-	-	-	1170

Oven (small convection) per m^3 of oven space	0.04-0.15 m^3	107000					1520
Open range (top), per 2 element section	2-10 elements	4100	1350				620
c) Gas, no hood required							
Broiler, per m^2 of broiling area	0.25	46600	190	16800	9030	25830	3840
d) Gas, Exhaust hood required							
Broiler, m^2 of broiling area	0.34-0.36 m^3	68900	1660	-	-	-	5690
Oven (bake deck), per m3 of oven space	0.15-0.46 m3	79400	190	-	-	-	1450
Range (burners), per 2 burner section	2-10 burners	9840	390	-	-	-	1930

Table 31 Household kitchen equipment energy rating. Source: CIBSE

Conclusions

This deliverable has shown the main factors that can influence the design of the heating storage system. These include climate variations across Europe, which determine different heating and cooling demands. Possible future demands using suitable assumptions were also calculated in order to anticipate how the system could respond in its implementation timeframe. This analysis shows a general decrease of future heating demands over Europe and an increase of future cooling needs, which is in agreement with the outcome of other studies.

The availability of solar energy in the continent was also studied, with a focus on the proposed demonstration sites. Although there is a marked difference between North and South in terms of overall solar radiation during the year, electrical outputs using conventional PV technologies still offer high possibilities continent-wide for their use in providing electrical supply.

The building stock in Europe has been analysed through the main characteristics. Key markets were identified, such as Germany, Spain, France, Italy, the United Kingdom and Poland. The dominating volumetric feature is that of apartment buildings, with most of the building stock being made between 1946 and 1990, with areas that range between 50 to 100 m². The most prevalent heating system is the central one. This means that future development of the MiniStor system involve that its effectiveness in most existing buildings will be greatly improved if it is offered as part of a building renovation package, whereas its effect might have certain limitations if those buildings are not well-insulated or with high infiltration rates. This needs to be corroborated at the demonstration and market feasibility study stages.

The influence of users and their activities within their dwellings was studied through abstractions made in standards and professional design guides. From the documentation available, the most comprehensive database preferred comes from ASHRAE as they have studied a wider variety of cases and with a high degree of detail. Although representing all possible usage cases is not possible, the most usual scenarios are given by these documents. An overview is given in the document of how and when users are present, the equipment they might use at a given time, and the energy levels involved from their use and activities performed which reflect as a minimum requirement that must be complied with to ensure comfort.

The outcomes from this deliverable will be used as basis for calculations to be performed in WP3, WP4 and WP5 to provide system specifications that will deliver a system that meets recommended standards and adapts to the climatic conditions of different European locations. These values will be corroborated during the demonstration stage (WP6). The level of detail that is necessary for a predictive system (WP5) will also be analysed based on the initial detail presented in this document. This deliverable also provides basic information that will be expanded in the market analysis and impact maximization stage (WP7).

References

ANSI/ASHRAE 2017. ANSI/ASHRAE Standard 55- Thermal Environmental Conditions for Human Occupancy. Atlanta, Georgia: ASHRAE.

ANSI/ASHRAE 2019a. ANSI/ASHRAE Standard 62.1-2019, Ventilation for acceptable Indoor air quality. Atlanta, Georgia: ASHRAE.

ANSI/ASHRAE 2019b. ANSI/ASHRAE Standard 62.2-2019, Ventilation and Acceptable Indoor Air Quality in Low-Rise Residential Buildings. Atlanta, Georgia: ASHRAE.

ANSI/ASHRAE 2019c. ANSI/ASHRAE Standard 90.1- Energy standard for buildings except low-rise residential buildings. Atlanta, Georgia: ASHRAE.

ARENDT, K. 2012. *Influence of external walls' thermal capacitance on indoor thermal comfort*. PhD thesis, Politechnika Gdańska.

ASHRAE 2017. *Handbook of Fundamentals*, Atlanta, Georgia.

AUTODESK. 2019. *Occupancy Schedules Revit products* [Online]. Available: https://knowledge.autodesk.com/support/revit-products/learn-explore/caas/CloudHelp/cloudhelp/2015/ENU/Revit-Analyze/files/GUID-D72DDB68-621C-4258-96FE-BEAD337B960E-htm.html [Accessed February 2020 2020].

AZEVEDO, J. A., CHAPMAN, L. & MULLER, C. L. 2015. Critique and suggested modifications of the degree days methodology to enable long-term electricity consumption assessments: a case study in Birmingham, UK. 22, 789-796.

BIZEE SOFTWARE - BUSINESS ENERGY EFFICIENCY SOFTWARE. 2019. *Degree Days.net - Custom Degree Day Data* [Online]. Available: https://www.degreedays.net/ [Accessed].

BUTCHER, K., CRAIG, B. & CHARTERED INSTITUTION OF BUILDING SERVICES ENGINEERS 2015. *Environmental design : CIBSE guide A*, London, Chartered Institution of Building Services Engineers.

CEN 2017. CEN standard 15193-1 Energy performance of buildings. Energy requirements for lighting. Specifications, Module M9. Brussels: European Committee for Standardization.

CIBSE 2006. *Degree-days: theory and application. Technical Manual 41.Chartered Institution of Building Services Engineers: London,UK. ISBN-10: 1-903287-76-6.*

COPERNICUS. *CORDEX regional climate model data on single levels for Europe* [Online]. Available: https://cds.climate.copernicus.eu/cdsapp#!/dataset/projections-cordex-single-levels?tab=overview [Accessed 2019-08-27].

DIFFENBAUGH, N. S., PAL, J. S., GIORGI, F. & GAO, X. 2007. Heat stress intensification in the Mediterranean climate change hotspot. 34.

EU COMMISSION 2019. Commission Recommendation (EU) 2019/786 of 8 May 2019 on building renovation Official Journal of the European Union.

EUROSTAT 2019. EU legislation on the 2021 population and housing censuses. Explanatory Notes. Luxembourg: Publications Office of the European Union.

GAGLIA, A., DIALYNAS, E. N., ARGIRIOU, A., KOSTOPOULOU, E., TSIAMITROS, D., STIMONIARIS, D. & LASKOS, K. 2018. Energy Performance of European Residential Buildings: Energy Use, Technical and Environmental Characteristics of the Greek Residential Sector – Energy Conservation and CO_2 Reduction. *Energy and Buildings*, 183, 86-104.

HELLENIC STATISTICAL AUTHORITY. Athens 2015. *2011 Buildings Census* [Online]. Available: http://www.statistics.gr/el/2011-census-pop-hous [Accessed March 2020].

HITCHIN, E. R. & HYDE, A. J. 1979. The estimation of heating energy use in buildings. *Proc. Symp. Environment Inside Building, Institute of Mathematics and its Applications*.

HORANYI, A. *Overview of regional climate projections* [Online]. Available: https://confluence.ecmwf.int/display/COPSRV/Overview+of+regional+climate+projections [Accessed].

HOTMAPS PROJECT. 2019. *Hotmaps Interface* [Online]. Available: https://www.hotmaps.hevs.ch/map [Accessed February 2020 2020].

IPCC 2014a. Climate Change 2014: Impacts, Adaptation, and Vulnerability. Part B: Regional Aspects. Contribution of Working Group II to the Fifth Assessment Report of the Intergovernmental

Panel on Climate Change. Cambridge University Press, Cambridge, United Kingdom and New York, NY, USA.

IPCC 2014b. Climate Change 2014: Synthesis Report. Contribution of Working Groups I, II and III to the Fifth Assessment Report of the Intergovernmental Panel on Climate Change. *In:* PACHAURI, R. K. (ed.). Geneva, Switzerland.

ISAAC, M. & VUUREN, D. 2009. Modeling global residential sector energy demand for heating and air conditioning in the context of climate change. *Energy Policy*, 37, 507-521.

KADIOĞLU, M., ŞEN, Z. & GÜLTEKIN, L. 2001. Variations and Trends in Turkish Seasonal Heating and Cooling Degree-Days. *Climatic Change*, 49, 209-223.

KOTTEK, M., GRIESER, J., BECK, C., RUDOLF, B., RUBEL, F. 2006. World Map of the Köppen-Geiger climate classification updated. *Meteorologische Zeitschrift*, 15, 259-263.

METEONORM. 2020. *Meteonorm Timeseries* [Online]. Available: https://meteonorm.com/en/meteonorm-timeseries [Accessed February 2020].

MOURSHED, M. 2012. Relationship between annual mean temperature and degree-days. *Energy and Buildings*, 54, 418-425.

PAPAKOSTAS, K., MAVROMATIS, T. & KYRIAKIS, N. 2010. Impact of the ambient temperature rise on the energy consumption for heating and cooling in residential buildings of Greece. *Renewable Energy*, 35, 1376-1379.

PEEL, M. C., FINLAYSON, B. L. & MCMAHON, T. A. 2007. Updated world map of Köppen-Geiger climate classification. *Hydrology and Earth System Sciences*, 439-473.

PVGIS. 2020. *Photovoltaic Geographical Information System* [Online]. Available: https://ec.europa.eu/jrc/en/pvgis [Accessed February 2020].

PVSYST. 2019. *PVSyst 6 Help* [Online]. Available: https://www.pvsyst.com/help/index.html?meteo_source_meteonorm.htm [Accessed February 2020 2020].

ROUSSELOT, M. E. 2018. *Energy efficiency trends in buildings* [Online]. Available: https://www.odyssee-mure.eu/publications/policy-brief/buildings-energy-efficiency-trends.html [Accessed June 2018].

SIA 2015. SIA bulletin 2024, Conditions d'utilisation standard pour l'energie et les installations du batiment. SIA - Swiss Society of Engineers and Architects.

SKARBIT, N., STEWART, I. D., UNGER, J. & GÁL, T. 2017. Employing an urban meteorological network to monitor air temperature conditions in the 'local climate zones' of Szeged, Hungary. 37, 582-596.

SPINONI, J., VOGT, J. & BARBOSA, P. 2015. European degree-day climatologies and trends for the period 1951–2011. 35, 25-36.

SPINONI, J., VOGT, J. V., BARBOSA, P., DOSIO, A., MCCORMICK, N., BIGANO, A. & FÜSSEL, H.-M. 2018. Changes of heating and cooling degree-days in Europe from 1981 to 2100. 38, e191-e208.

THERMAL ENERGY SYSTEM SPECIALISTS. 2019. *TRNSYS Energy Simulation Software* [Online]. Available: http://www.trnsys.com/index.html [Accessed].

THOMSON, A. M., CALVIN, K. V., SMITH, S. J., KYLE, G. P., VOLKE, A. C., PATEL, P. L., DELGADO ARIAS, S., BOND-LAMBERTY, B., WISE, M. A., CLARKE, L. E. & EDMONDS, J. A. 2011. RCP4.5: A Pathway for Stabilization of Radiative Forcing by 2100.

U.S. DEPARTMENT OF ENERGY. 2020. *EnergyPlus weather* [Online]. Available: https://energyplus.net/weather [Accessed].

VAN VUUREN, D. P., EDMONDS, J., KAINUMA, M., RIAHI, K., THOMSON, A., HIBBARD, K., HURTT, G. C., KRAM, T., KREY, V., LAMARQUE, J.-F., MASUI, T., MEINSHAUSEN, M., NAKICENOVIC, N., SMITH, S. J. & ROSE, S. K. 2011. The representative concentration pathways: an overview. *Climatic Change*, 109, 5.

WIKIPEDIA. *Unified degree day* [Online]. Available: https://fr.wikipedia.org/wiki/Degr%C3%A9_jour_unifi%C3%A9 [Accessed May 30, 2019].